Research Square

Preprints are preliminary reports that have not undergone peer review.
They should not be considered conclusive, used to inform clinical practice,
or referenced by the media as validated information.

Regional seismic site response assessment in the deep Bengal Basin, Bangladesh, from simulated far-field earthquake ground motions

Atikul Haque Farazi
ahfarazi@bu.ac.bd
University of Barishal
José Piña-Flores
Universidad Veracruzana
Md. Shakhawat Hossain
University of Dhaka
Nasim Ferdous
Environmental and Geospatial Solutions
Sukhen Goswami
University of Barishal
Md Wabidur Rahman
University of Barishal

Research Article

Keywords: Engineering bedrock depth, Elastic response spectrum, Frequency-dependent amplification, Seismic soil classification, Thick soft sediments, Bangladesh National Building Code (BNBC)

Posted Date: September 8th, 2026

DOI: https://doi.org/10.21203/rs.3.rs-10756765/v1

License: This work is licensed under a Creative Commons Attribution 4.0 International License.
Read Full License

Additional Declarations: No competing interests reported.

Regional seismic site response assessment in the deep Bengal Basin, Bangladesh, from simulated far-field earthquake ground motions

Atikul Haque Farazi[1]*, José Piña-Flores[2], Md. Shakhawat Hossain[3], Nasim Ferdous[4], Sukhen Goswami[1], Md Wabidur Rahman[1]

[1]Department of Geology and Mining, University of Barishal, Barishal-8254, Bangladesh.

[2]Instituto de Ingeniería, Universidad Veracruzana, Xalpa, Veracruz 94292, México.

[3]Department of Disaster Science and Climate Resilience, University of Dhaka, Dhaka-1000, Bangladesh.

[4]Environmental and Geospatial Solutions, Dhaka-1000, Bangladesh.

Corresponding Author: Atikul Haque Farazi, Department of Geology and Mining, University of Barishal, Barishal 8254, Bangladesh, Email: ahfarazi@bu.ac.bd. Md. Shakhawat Hossain, Department of Disaster Science and Climate Resilience, University of Dhaka, Bangladesh, Email: shakhawat.dsm@du.ac.bd.

Orchid ID: Atikul Haque Farazi (https://orcid.org/0000-0002-1822-1421), José Piña-Flores (https://orcid.org/0000-0002-4046-0322), Md. Shakhawat Hossain (https://orcid.org/0000-0002-0205-2846), Sukhen Goswami (https://orcid.org/0009-0007-8342-6822), Md Wabidur Rahman (https://orcid.org/0009-0002-6313-1510).

Acknowledgements

This research was supported by the Special Research Grant (2025–2026) from the Ministry of Science and Technology, Government of the People's Republic of Bangladesh (Grant ID: SRG-252373). The authors gratefully acknowledge the Department of Geology and Mining, University of Barishal, for its support in conducting this research. We are also indebted to Creative Soil Investigation for performing the sub-soil investigations through SPT borings.

The authors used ChatGPT (OpenAI) to improve the English language throughout the manuscript.

Abstract

Bangladesh is vulnerable to large earthquakes because of its location within the active Eurasia–India–Burma plate tectonic system and the widespread occurrence of thick soft sediments across the Bengal Basin. The long-period shaking of high-rise buildings in the Bangkok Basin during the 2025 M_W 7.7 Myanmar earthquake highlighted the importance of understanding the response of deep sedimentary basins to far-field earthquakes. In Bangladesh, the Bangladesh National Building Code (BNBC) adopts V_{S30} based seismic site characterization, where the influence of deep, soft sedimentary sequences on site response remains undermined. This study presents the regional assessment of seismic site response in terms of elastic response spectrum at nineteen sites across the Bengal Basin using one-dimensional (1D) linear simulations of two far-field earthquake ground motions and deep shear-wave (S-wave) velocity (V_S) profiles derived from a previous horizontal-to-vertical spectral ratio (HVSR) inversion study. Rather than quantifying absolute amplification, the study investigates the predominant response periods associated with the deep sedimentary sequences of Bangladesh. The reliability of the velocity models was evaluated through comparison with standard penetration test (SPT) based site classifications. Many stations exhibited dominant spectral periods approaching 1 s, exceeding the peak periods of the BNBC design spectra, with engineering bedrock depth being a controlling factor on the dominant site response period. This study shows that the deep soft sediments of Bangladesh have the potential to amplify long-period ground motions from far-field earthquakes, suggesting that the traditional V_{S30} based seismic site characterization alone is insufficient here and should incorporate engineering bedrock depth.

Keywords: Engineering bedrock depth, Elastic response spectrum, Frequency-dependent amplification, Seismic soil classification, Thick soft sediments, Bangladesh National Building Code (BNBC).

Article Highlights

- First regional attempt to explore far-field earthquake effects in the deep sedimentary Bengal Basin.
- Long-period site response may extend beyond the periods represented in BNBC (2020) design spectra.

- Dominant site response period varies systematically with engineering bedrock depth.

1. Introduction

Earthquakes are among the deadliest natural hazards, capable of causing severe casualties and catastrophic structural damage worldwide. The severity of earthquake damage depends not only on earthquake magnitude, rupture characteristics, and seismic wave propagation paths but also on local site conditions that modify incoming ground motions before they reach the Earth's surface (Borcherdt, 1994; Street et al., 1997). Moreover, shaking amplified by basin resonance (Bard & Gariel, 1986; Theodoulidis et al., 2017), and soil-structure interaction (Gallipoli et al., 2004) may elevate the destruction. Numerous destructive earthquakes, including the 1985 Mexico City, 1995 Kobe, 1999 Chi-Chi, and 2011 Tohoku earthquakes, have demonstrated that local geological conditions can potentially amplify seismic waves, alter their frequency content, shaking duration to increase structural damage (Borcherdt, 1994; Kaklamanos et al., 2015). Recently, the 2025 M_W 7.7 Myanmar supershear earthquake produced severe, long-period shaking in the Bangkok Basin, located approximately 600 km from the epicenter, causing significant oscillation in high-rise buildings and the collapse of a high-rise structure (Ornthammarath et al., 2025; Pananont et al., 2026). Amplification of long-period far-field earthquake ground motions in sedimentary basins has also been reported in other regions of the world (Berge-Thierry et al., 2001; Cruz-Atienza et al., 2016; Furumura & Kennett, 2019). This phenomenon demonstrates the importance of understanding the far-field earthquake ground motions on thick sedimentary basins like the Bengal Basin in Bangladesh.

Seismic site characterization is a fundamental component of seismic hazard assessment and preparedness because it quantifies how local geological and geotechnical conditions modify earthquake ground motions as seismic waves propagate from engineering bedrock to the ground surface (Chopra, 1995). In conventional seismic hazard assessment approaches, regional ground motion predictive equations (GMPEs) or probabilistic seismic hazard assessments (PSHA) generally compute expected ground shaking at a standard engineering bedrock datum. However, executing a comprehensive seismic risk mitigation strategy requires mapping hazards at the ground surface, where civil infrastructure resides. This transition necessitates a robust evaluation of site response, which quantifies the frequency-dependent amplification and resonance phenomena induced by overlying soil columns (Rathje et al., 2010).

Site response is commonly characterized by the amplification of earthquake ground motion and the frequency of the dominant amplification. These properties can be evaluated using empirical approaches, such as the horizontal-to-vertical spectral ratio (HVSR) method (Janusz et al., 2025; S. Molnar et al., 2018; Wu et al., 2026), site coefficients based on V_{S30} (Borcherdt, 1994), numerical site-response analyses, and analyses of recorded earthquake ground motions (Chowdhury et al., 2024; Wu et al., 2026). Owing to its simplicity, V_{S30} has become the standard parameter for seismic site classification in the National Earthquake Hazards Reduction Program (NEHRP) (Street et al., 1997, 2001), Eurocode 8 (Lontsi et al., 2026; Pitilakis et al., 2019), and the Bangladesh National Building Code (BNBC, 2020). However, several studies have shown that V_{S30} alone cannot adequately represent site amplification in deep sedimentary basins where engineering bedrock commonly occurs well below 30 m (Farazi et al., 2023; Manea et al., 2020; Rahman et al., 2021). Numerical site-response analyses, predominantly based on 1D equivalent-linear or nonlinear wave-propagation models, remain a widely accepted engineering approach because of their computational efficiency and reliance on vertically propagating S-waves through layered media (Kramer & Stewart, 2024; Seed et al., 1972). Although deep sedimentary basins may exhibit multidimensional wave scattering and basin-edge effects (Bard & Bouchon, 1985), 1D analyses still provide a practical basis for site-specific seismic hazard assessment.

Where strong-motion observations are limited, realistic surface ground motions can be estimated by propagating earthquake motions recorded at a suitable hard-rock reference site through transfer functions derived from site-specific V_S profiles (Molnar et al., 2022; Ordaz & Montoya, 2000; Wu et al., 2026). This approach enables the generation of synthetic ground motions and elastic response spectra while explicitly accounting for local geological conditions, making it particularly suitable for regional seismic hazard assessment in data-limited sedimentary basins such as the Bengal Basin.

Bangladesh occupies the major part of the Bengal Basin, one of the world's largest and deepest sedimentary basins (Alam et al., 2003; Bürgi et al., 2021), and is in a tectonically active region influenced by the ongoing convergence of the Indian, Eurasian, and Burma plates (Bilham, 2004; Molnar & Tapponnier, 1975; Steckler et al., 2008). The country is bounded by the Himalayan tectonic system to the north and the Indo-Burmese subduction system to the east, while active structures such as the Dauki Fault, and the Chittagong Tripura-Tripura Fold Belt (CTFB) further contribute to the regional seismic hazard (Bilham, 2004; Morino et al., 2011; Steckler et al., 2016) (Fig. 1). Historical earthquakes, including the 1762 Arakan, 1869 Cachar,

1885 Bengal, 1897 Great Assam, 1918 Srimangal, 1934 Bihar–Nepal, and the 2015 Gorkha Nepal earthquakes, demonstrate that Bangladesh is vulnerable to strong ground shaking generated by both nearby and regional seismic sources (Bilham & Hough, 2006; Lizundia et al., 2017; Oldham, 1899). Rapid urbanization, increasing population density, and widespread infrastructure development over thick unconsolidated sediments have further increased the country's seismic risk (Hossain et al., 2020; Rahman et al., 2015; Rahman, et al., 2018). Therefore, understanding how the geological conditions of the Bengal Basin influence the propagation and amplification of earthquake ground motions is essential for realistic seismic hazard assessment and earthquake-resistant structural design in Bangladesh.

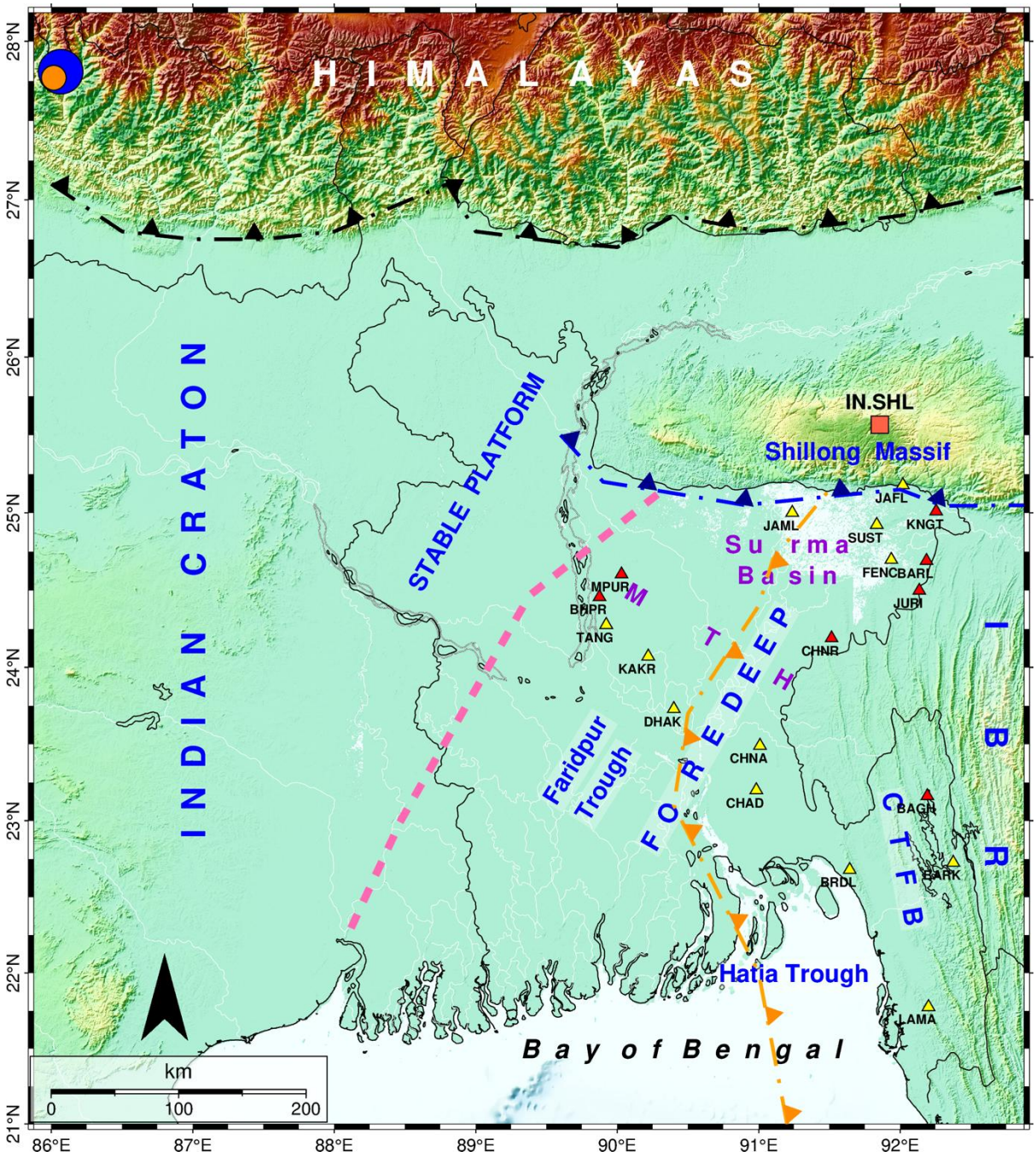


Figure 1. Map showing tectonic elements in and around the Bengal Basin along with the distribution of the seismic stations from where the V_S profiles of Farazi et al. (2023) were taken in this study and subsequently site response was estimated. The yellow triangles indicate station locations with nearby SPT boreholes, while the red triangles indicate those without a borehole. The red square symbolizes station SHL for the site response study. The blue and orange circles indicate the locations of the M_W 7.3 and 6.7 earthquakes, respectively (Table 2). The blue dashed dotted line indicates the Dauki fault. The orange dashed dotted line indicates the inferred Indo-Burmese plate boundary thrust. The black dashed line indicates the Indo-Eurasian plate boundary thrust. The triangle direction with these lines indicates the subduction direction. Pink dashed line indicates the Eocene Hinge Zone. The triangles indicate the seismic stations with the station code given in the text below. The orange color star denotes Dhaka, the capital city of Bangladesh. CTFB: Chittagong Tripura fold belt; IBR: Indo-Burmese ranges; FT: Faridpur trough; HT: Hatiya Trough; MTH: Madhupur Tripura High. The tectonic elements are from Alam et al. (2003) and Steckler et al. (2016).

Several studies have investigated seismic site characterization and site response in Bangladesh using geophysical, geotechnical, and numerical approaches. Early investigations primarily focused on seismic microzonation and site amplification using borehole information, SPT data, ambient vibration measurements, and site response analyses for major urban areas such as Dhaka, Sylhet, Chittagong, etc. (Ansary et al., 2004; Ansary & Arefin, 2019; Rahman et al., 2016; Rahman, et al., 2018; Rahman, et al., 2018). More recent studies have incorporated multichannel analysis of surface waves (MASW), P- and S-wave (PS) logging, HVSR analysis, equivalent-linear and nonlinear site response analyses, and comparisons with the BNBC (2020) to improve the estimation of site-specific ground motions and response spectra (Hossain et al., 2023; Mitu et al., 2025; Rahman et al., 2021; Zaman et al., 2026). Additionally, PSHA and updated seismic source models have improved the characterization of regional seismic sources and expected bedrock ground motions regionally for Bangladesh (Rahman et al., 2025; Samm-A et al., 2025). Although these studies have advanced the understanding of seismic hazard in Bangladesh, most of them, except the study of Rahman et al. (2021), primarily relied on shallow subsurface characterization or V_{S30} based site classification. In Bangladesh, the BNBC (2020) estimates seismic site class and related design spectra regionally based primarily on the V_{S30}, SPT resistance, and undrained shear strength employing the PSHA approach. While this framework provides a practical representation of near-surface soil stiffness, it underestimates the influence of deep sedimentary structure as well as long-period ground-motion amplification

(Zaman et al., 2026), which may be significant in thick sedimentary basins such as the Bengal Basin.

Recently, Farazi et al. (2023) performed the first HVSR inversion study regionally in the Bengal Basin using ambient noise measurements from nineteen seismic stations to estimate deep shear-wave velocity profiles and engineering bedrock depths. Their results demonstrated that engineering bedrock commonly occurs well below 30 m throughout much of the basin, suggesting that conventional V_{S30} based site classification alone may not adequately represent the dynamic response of these thick sedimentary deposits. They further demonstrated the applicability of the derived velocity models through site-response analysis at a representative station (DHAK), where the predominant spectral period was approximately 0.8–1.0 s. Another study by Rahman et al. (2021) demonstrated that the engineering bedrock depth below Dhaka City is at >100 m. They also showed, using response spectrum estimation, that short-period ground motions are deamplified due to thick sediments, while long-period ones are amplified. Referring to the historical record of destruction caused to multi-story buildings due to distant earthquakes, they raised concern about the potential effect of far-field ground motion in Dhaka City by amplifying long-period ground motion to cause damage to high-rise buildings. Nevertheless, a comprehensive regional assessment of seismic site amplification using these deep velocity profiles has not yet been undertaken. In particular, the spatial variability of transfer-function characteristics, peak ground acceleration (PGA), pseudo-spectral acceleration (PSA), predominant response period, and their relationships with engineering bedrock depth and conventional V_{S30} based site classification remain largely unexplored across the Bengal Basin.

The recent observation from the Bangkok Basin following the 2025 M_W 7.7 Myanmar earthquake emphasize the importance of understanding how thick sedimentary basins respond to distant large earthquakes. Like the Bangkok Basin, large parts of Bangladesh are underlain by thick, soft sediments capable of producing strong long-period shaking from large earthquakes originating along the Himalayan and Indo-Burmese tectonic systems. However, the scarcity of suitable broadband strong-motion recordings from nearby large earthquakes makes direct evaluation of regional site amplification difficult. Consequently, investigating far-field earthquake response using simulated ground motions offers a practical, physically consistent approach to evaluating potential long-period amplification and regional variations in seismic site response throughout the Bengal Basin.

Seismic hazard assessment in Bangladesh has primarily focused on peak ground acceleration (PGA), V_{S30} based site classification, and design spectrum coefficients adopted in the BNBC (2020). Consequently, the predominant response period, which governs the potential for resonance between earthquake ground motions and structures, has received comparatively little attention. Therefore, this study focuses primarily on identifying the predominant spectral period associated with the deep sedimentary structure of the Bengal Basin rather than quantifying absolute amplification levels.

This study presents the first regional assessment of seismic site response across the Bengal Basin using one-dimensional (1D) linear simulations of two far-field subduction-zone earthquakes and deep shear-wave velocity (Vs) profiles derived from the HVSR inversion of Farazi et al. (2023). Because HVSR inversion is inherently non-unique, the reliability of the adopted velocity models was evaluated by comparing the resulting V_{S30} based seismic site classifications with those independently obtained from SPT borehole data. The study then investigates the regional variability of elastic response spectra with respect to seismic site classification and the BNBC (2020) design spectra, and further examines the influence of engineering bedrock depth on the dominant ground-motion period and site amplification across the Bengal Basin. Motivated by the widespread long-period shaking observed in the thick sedimentary Bangkok Basin during the 2025 M_W 7.7 Myanmar supershear earthquake, this study primarily focuses on the dominant elastic response period, rather than absolute amplification levels or PGAs, to investigate the potential of the deep soft sediments of the Bengal Basin to amplify long-period ground motions generated by far-field earthquakes. The findings of this study will provide valuable insights into the control of thick, soft soil on regional seismic site response and contribute to encourage improved seismic hazard assessment, site-specific ground-motion characterization, and earthquake-resistant design in Bangladesh considering long-period ground motion typical of a thick sedimentary basin.

2. Study Area

2.1. Geological Setting

The Bengal Basin, occupying most of Bangladesh and extending into eastern India, is a pericratonic foreland basin along the eastern margin of the Indian Plate (Alam et al., 2003). With sedimentary successions reaching approximately 20–22 km in thickness (Mitra et al.,

2018; Singh et al., 2016), it is one of the world's largest and deepest sedimentary basins. The basin lies at the junction of the Indian, Eurasian, and Burma plates, resulting in a complex tectonic framework. The megathrust fault of the Indo-Burmese subduction system is inferred to extend beneath the eastern part of the basin (Steckler et al., 2008, 2016). Unlike most active subduction zones, the Bengal Basin is filled with enormous volumes of sediments transported from the Himalayas by the Ganges–Brahmaputra–Meghna (GBM) river system, forming one of the world's largest deltaic plains (Najman et al., 2008; Steckler et al., 2008).

The basin is bounded by the Shillong Massif to the north, the Indian Craton to the west, the Indo-Burmese Ranges to the east, and continues southward into the Bay of Bengal (Mitra et al., 2006). It is subdivided into three principal tectonic provinces: the Stable Shelf, the Bengal Foredeep, and the Chittagong-Tripura Fold Belt (CTFB, Fig. 1). The Bengal Foredeep occupies the central part of the basin and consists of several tectonically controlled sub-basins, including the Surma Basin (Sylhet Trough), Faridpur Trough, and Hatia Trough, which supposedly formed through continued subsidence and intrabasinal faulting associated with the ongoing convergence of the surrounding tectonic plates (A. A. Khan & Chouhan, 1996). The Madhupur and Comilla tracts represent uplifted structural highs that separate the sub-basins (Goodbred et al., 2003).

The Surma Basin in northeastern Bangladesh contains up to approximately 25 km thick sedimentary sequences (Johnson & Alam, 1991). Its northern boundary is defined by the active Dauki Fault, along which uplift of the Shillong Massif since the Late Miocene has been accompanied by continued subsidence within the foreland basin (Alam et al., 2003). East of the foredeep, the CTFB forms a series of north–south-trending anticlines and synclines produced by active deformation above the Indo-Burmese subduction system (Khan and Chouhan, 1996). This province represents the westernmost expression of the Indo-Burmese Ranges and exhibits markedly different topography and structural style from the relatively flat foredeep, with elevations increasing eastward to approximately 1500 m (Bürgi et al., 2021).

The seismic stations considered in this study are distributed across the Bengal Foredeep and the CTFB tectonic provinces of the Bengal Basin (Fig. 1); therefore, the present investigation is confined to these structurally active regions. The deep basin comprises a thick sedimentary succession ranging in age from the Cretaceous to the Holocene (Alam et al., 2003). Within the study area, however, the shallow to intermediate subsurface is predominantly composed of Miocene to Holocene sedimentary sequences (Farazi et al., 2023). The upper several hundred meters generally consist of unconsolidated to weakly consolidated Holocene alluvial deposits

together with the fluvial Dihing and Dupi Tila formations, which are dominated by loose- to medium-grained sands with interbedded silts and clays. Owing to the dynamic depositional history of the GBM river system, the local stratigraphy exhibits considerable lateral facies variations and heterogeneity over relatively short distances (Small et al., 2009).

2.2. Seismotectonic Setting

The Bengal Basin in Bangladesh formed by the northward collision of the Indian Plate with the Eurasian Plate and subsequent sedimentation from the Himalayan River systems (Aitchison et al., 2019; Alam et al., 2003; Najman et al., 2008; Rao et al., 1994). The country is bounded by the actively converging Himalayan and Indo-Burman tectonic systems, making it prone to earthquakes generated by regional plate boundary faults and crustal fault systems (Maurin & Rangin, 2009; Steckler et al., 2008). Major active structures surrounding Bangladesh include the Dauki Fault to the north, the Indo-Burman subduction zone to the east, and the Sagaing Fault in Myanmar, all of which have generated large historical earthquakes affecting the region (Morino et al., 2011; Oldham, 1899; Szeliga et al., 2010). The regional seismotectonic setting together with the major active faults and historical earthquakes is shown in Figure 2. Based on BNBC (2020), the country is divided into four seismic zones (Zones I–IV) with design peak ground accelerations (PGA) of 0.12 g, 0.20 g, 0.28 g, and 0.36 g, respectively, with the northeastern region assigned the highest seismic hazard (Fig. 3). The nineteen seismic stations considered in this study are distributed across these seismic zones, providing representative coverage of the major geological and tectonic settings of Bangladesh.

3. Data

This study was conducted at 19 seismic stations sites across the Bengal Basin (Fig. 1), where 1D V_S profile up to around 3000 m depth was estimated by Farazi et al. (2023) by inverting noise HVSR. In this study, elastic site response spectrum was estimated using parameters of each site from these profiles, including P-wave velocity (V_P), S-wave velocity (V_S), density, and Poisson's ratio.

A reference hard-rock site is required to estimate the incoming bedrock ground motion for regional site response analysis. For this purpose, station SHL, located in Shillong, Meghalaya, India (Fig. 1), was selected because it is situated on competent hard rock (Sadiq et al., 2018) and is currently the only openly available broadband seismic station in the vicinity of the

Bengal Basin. The station is operated by the India Meteorological Department under the IN seismic network (https://www.fdsn.org/networks/detail/IN/). Owing to the limited availability of suitable broadband recordings at SHL, only two large-magnitude regional earthquakes were available for the present analysis during the station's operational period.

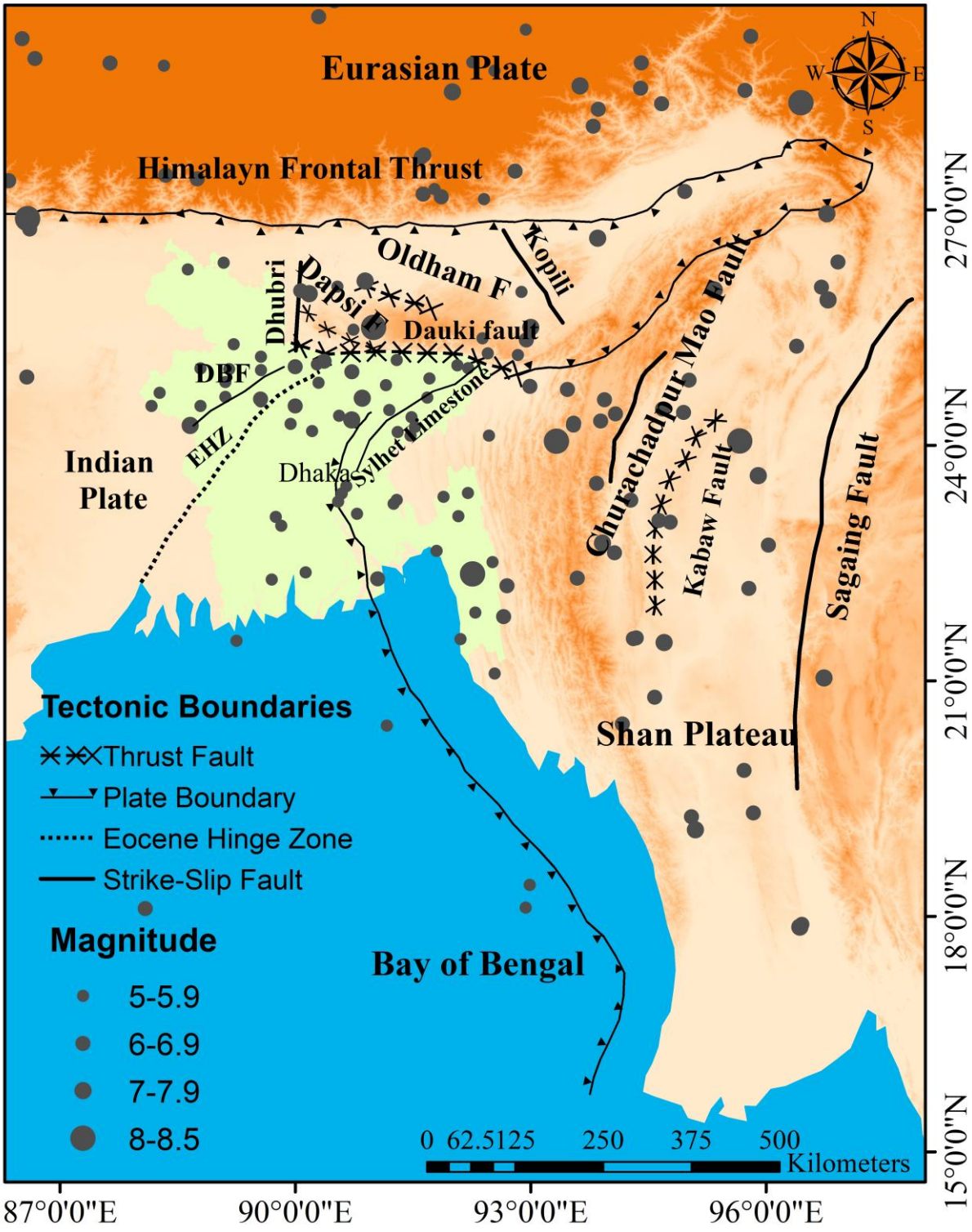


Figure 2. Seismotectonic map of Bangladesh and surrounding regions exhibiting historical earthquakes. The earthquake data are taken from Ambraseys & Douglas (2004), Szeliga et al. (2010) and United States Geological Survey (USGS, https://earthquake.usgs.gov/earthquakes/search/). The map is modified from Kamal et al. (2021).

Two regional subduction-zone earthquakes (Table 1) that occurred in Nepal and were recorded at station SHL were selected as the input motions for this study (Table 2). Both earthquakes are aftershocks of the M_W 7.8 Gorkha earthquake sequence (Lizundia et al., 2017) and represent the largest suitable subduction-zone events available in the SHL archive. Because large local subduction-zone earthquake recordings are unavailable within or adjacent to the Bengal Basin, these earthquake records provide the most appropriate observed input motions for simulating regional seismic site response in the study area.

Table 1. Description of the seismic events used for site effect estimation. Source: USGS (https://earthquake.usgs.gov/earthquakes/search/).

Event date	GMT time	Lat	Long	Depth (km)	Magnitude (M_W)
2015-04-26	07:09:10	27.77	86.02	22.9	6.7
2015-05-12	07:05:19	27.81	86.07	15	7.3

Table 2: Information of reference site's seismic station SHL.

Station Code	Site	Lat	Long	Sensor	Sampling Frequency (Hz)
SHL	Shillong, Meghalaya, India	25.566816	91.855949	Broadband	100

For seismic soil classification at each seismic station, the site-specific subsurface velocity models previously developed by Farazi et al. (2023) through ambient-noise HVSR inversion were adopted. But the results of this study were obtained by highly non-unique HVSR inversion. Therefore, to verify the reliability of site class estimation from this study, we also

estimated site class from Standard Penetration Test (SPT) boreholes nearby 12 seismic stations (Fig. 1). The SPT boreholes were completed to a depth of 30 m at or near each seismic station. This sub-soil investigation provides SPT-N value at each 1.5 m depth intervals from the ground surface and lithology of a site.

4. Methodology

In the present study, simulated earthquake ground motions derived from the broadband reference station SHL were used as the input motions for one-dimensional linear elastic site response analysis. This approach provides a consistent input ground motion for all study sites and overcomes limitations associated with the heterogeneous instrumentation of the Bangladesh seismic network, where some stations are equipped with intermediate-period sensors whereas others use short-period sensors. Consequently, the simulated ground motions preserve the long-period frequency content of the reference recordings, allowing the influence of deep sedimentary deposits on seismic site response to be evaluated. This is particularly important in the Bengal Basin, where engineering bedrock commonly occurs at depths far exceeding 30 m (Farazi et al., 2023; Rahman et al., 2021), making conventional Vs30-based approaches insufficient for characterizing long-period site amplification.

Although the selected earthquake records are far-field observations, with an epicentral distance of approximately 1162 km from the reference station SHL, they retain abundant long-period energy from subduction zone earthquake despite their relatively low amplitudes. Such ground motions are particularly suitable for investigating the linear elastic response of the deep sedimentary deposits underlying the Bengal Foredeep and the CTFB, where thick sedimentary successions preferentially amplify long-period seismic waves (Farazi et al., 2023; Furumura & Kennett, 2019; Rahman et al., 2021). The widespread long-period ground motions generated in the approximately 600 km distant Bangkok Basin during the 2025 MW 7.7 Myanmar earthquake (Ornthammarath et al., 2025; Pananont et al., 2026) further demonstrate the importance of evaluating the response of thick sedimentary basins to large regional earthquakes. Therefore, the selected earthquake records provide an appropriate basis for investigating the potential long-period seismic response of the Bengal Basin.

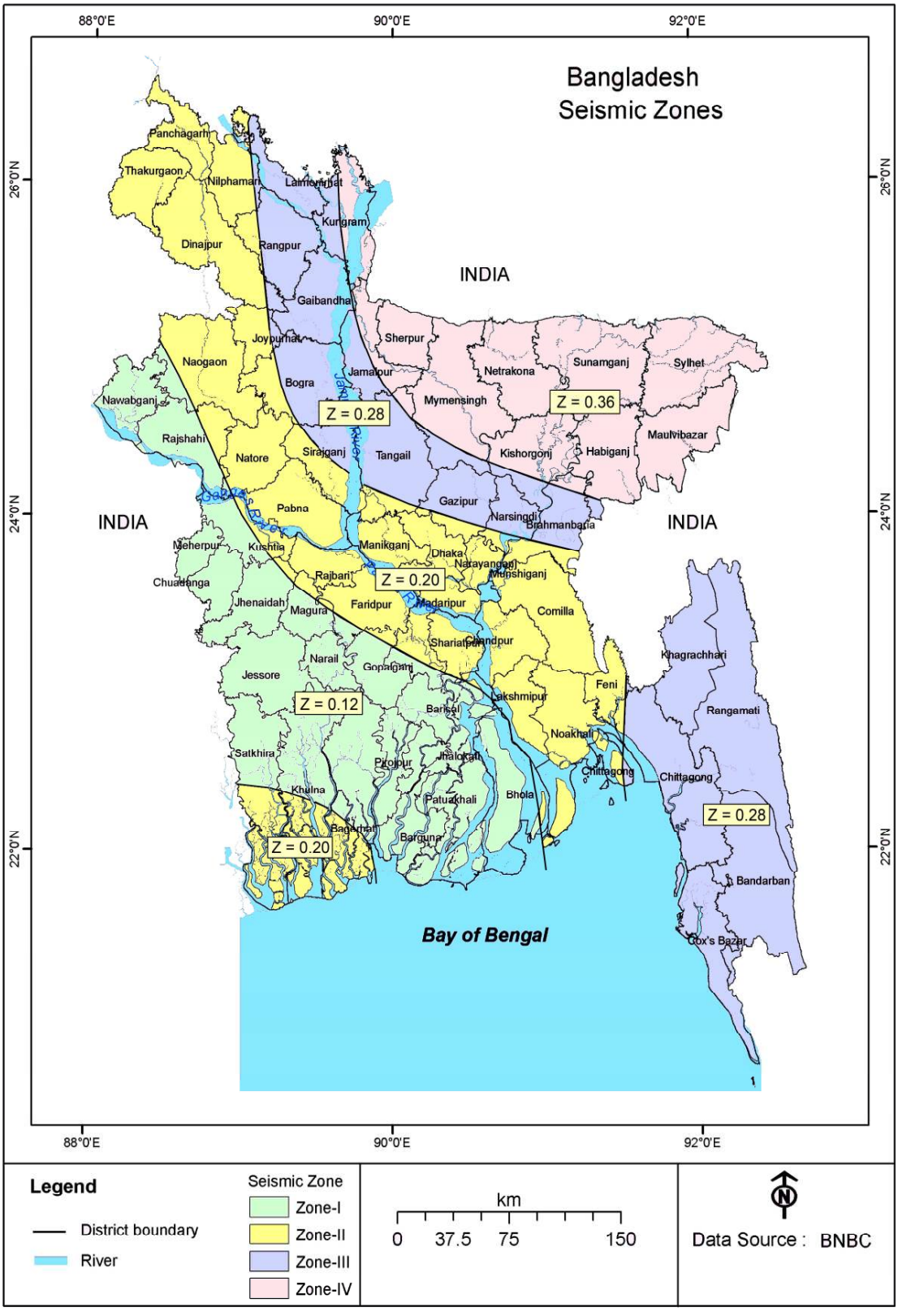


Figure 3. Seismic zonation map of Bangladesh (BNBC, 2020).

The earthquake records from the hard-rock reference station SHL, previously validated by Farazi et al. (2023) using earthquake HVSR analysis (Fig. 4), were adopted as the input motions

for this study. Only the east–west (EW) horizontal component was used for all site response simulations and elastic response spectrum calculations.

4.1. Computation of Elastic Response Spectrum

The seismic response spectra were computed at 19 seismic stations in Bangladesh using two scenario earthquakes (M_W 6.7 and 7.3) recorded at the reference station SHL (Fig. 1 and Table 2). In this study, only the east–west (EW) horizontal component of the recorded accelerograms was used throughout the analysis because it exhibited a high signal-to-noise ratio and provided a consistent reference record for all simulations. The workflow for spectral acceleration estimation is illustrated in Figure 4.

To incorporate local site effects, the recorded reference motion was modified using one-dimensional transfer functions computed for each station. The transfer function describes the frequency-dependent amplification or de-amplification of vertically incident horizontally polarized SH waves within the soil column (Molnar et al., 2022). This is ultimately a ratio between the motion at the surface and that in the bedrock. The transfer functions were computed using the reflectivity method (Kennett & Kerry, 1979) based on the layered velocity models developed in this study. Each soil profile consists of layer thickness, P-wave velocity (V_P), S-wave velocity (V_S), density, and the quality factors for P- and S-waves. Consequently, the computed transfer functions represent the Fourier transfer functions of vertically propagating SH waves. The transfer functions for all stations are presented in Figure 5.

Synthetic acceleration time histories were subsequently generated by convolving the Fourier spectrum of the reference earthquake with the corresponding site transfer function in the frequency domain, followed by inverse Fourier transformation. In this way, the simulated accelerograms incorporate the local site amplification effects at each station. The simulated accelerograms for all stations are shown in Figure 6.

The structural response to each simulated accelerogram was computed by solving the equation of motion of a damped single-degree-of-freedom (SDOF) oscillator (Chopra, 1995):

$$m\ddot{u}(t) + c\dot{u}(t) + f_s(u,\dot{u})(t) = -ma(t) \qquad (1)$$

where u, $\dot{u}$ and $\ddot{u}$ are the displacement, velocity and acceleration of the oscillator mass, respectively, at time t; $c\dot{u}(t)$ introduces damping into the above equation, influencing how the

structure would respond at different periods; f_s represents the resisting force at time t. According to Hooke's law, $f_s(u, \dot{u}) = -ku$, where k is the stiffness of the system. The resultant displacement curve is presented in terms of acceleration to obtain a pseudo-acceleration spectrum (PSA), which we will refer as the response spectrum for each site.

The elastic response spectrum was then calculated using the Degtra program (Ordaz & Montoya, 2000). Degtra determines the maximum oscillator response over a range of natural periods by evaluating the displacement energy of the oscillator,

$$E = \left| -m \int a(t) dx \right| \qquad (2)$$

where x is the relative oscillator displacement. Repeating the calculation over a continuous range of vibration periods produces the elastic response spectrum. The maximum oscillator displacements are finally expressed as equivalent pseudo-spectral accelerations (PSA), which are referred to as the response spectrum throughout this study. The resulting response spectra for all stations are presented in Figure 7.

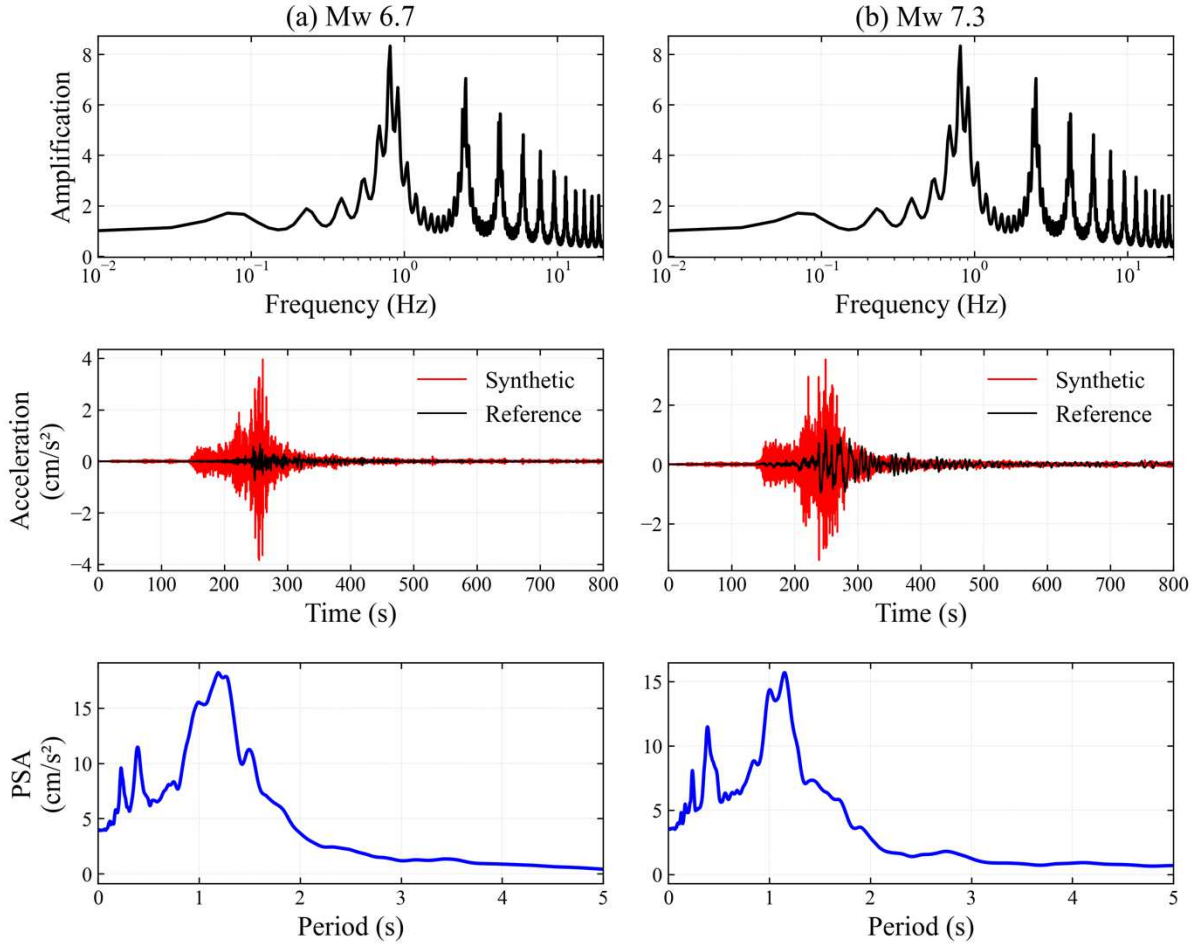


Figure 4. Illustration of the workflow for estimating site-specific pseudo-spectral acceleration (PSA) estimation at station BHPR for the Mw 6.7 (a) and Mw 7.3 (b) subduction earthquakes. The top panels show the one-dimensional SH-wave transfer functions computed from the site-specific velocity model. The middle panels compare the reference site's amplified accelerograms recorded at the hard-rock station SHL (black) with the corresponding synthetic accelerograms at BHPR (red), obtained by incorporating the site transfer function into the reference motion in the frequency domain. The bottom panels present the resulting 5%-damped pseudo-spectral acceleration (PSA). This workflow was applied to all seismic stations to evaluate regional variations in seismic site amplification across the Bengal Basin.

4.2.Seismic Site Class Estimation

The transfer functions and pseudo-spectral accelerations (PSA) in this study were computed using the complete V_S profiles obtained by inversion of ambient-noise HVSR data (Farazi et al., 2023). Therefore, seismic site classification was first performed using the V_{S30} values derived from these HVSR inversion profiles. To evaluate the reliability of the HVSR based site classification, geotechnical investigation boreholes with Standard Penetration Tests (SPT) was conducted at 12 sites (Fig. 1 and Table 4) at 1.5 m intervals to a depth of 30 m were used to independently estimate V_{S30}. The borehole logs indicate that the subsurface materials are predominantly composed of sand and clay, and an example SPT borehole log is presented in Figure 8. Since no established SPT–V_S correlation is currently available for Bangladesh as a whole, V_S were estimated using the empirical relationships developed for Dhaka soils (Shehab, 2015). The regression equations for sandy and clayey soils developed for Dhaka soils are given by:

$$V_S = 147N^{0.19} \quad (3)$$

$$V_S = 84N^{0.30} \quad (4)$$

where N denotes the uncorrected field SPT-N value. The resulting V_{S30} values were subsequently used to assign seismic site classes according to the BNBC (2020) classification criteria based on SPT-N value (Table 3). Herein, the V_{S30} was calculated using the harmonic mean of the layer velocities, which accounts for the travel time of seismic waves through individual layers. The equation is:

$$V_{S30} = \frac{30}{\sum_{i=1}^{n} \frac{h_i}{V_{S,i}}} \quad (5)$$

where, h_i denotes the thickness of the i-th layer (m), $V_{S,i}$ is the S-wave velocity of the i-th layer (m/s), and the summation is performed over all layers within the upper 30 m. The site classifications obtained from the HVSR-derived V_{S30} (Farazi et al., 2023), V_{S30} of the Dhaka soil correlations (Shehab, 2015), and the BNBC (2020) classification are summarized in Table 4.

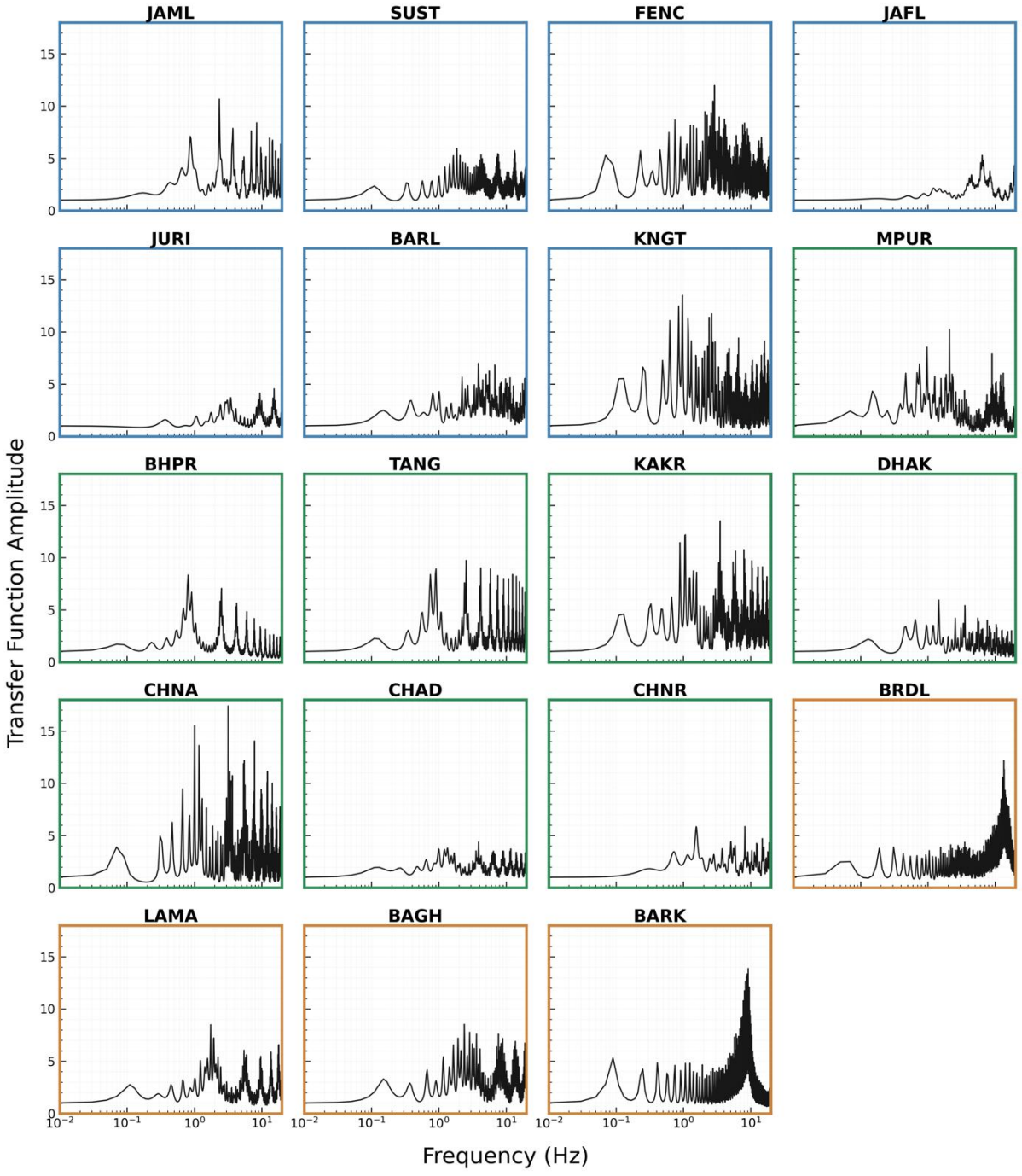


Figure 5. One-dimensional SH-wave transfer functions computed for the 19 seismic stations used in this study. Stations are grouped according to their tectonic setting, namely the Surma Basin (blue panels), Central Bengal Foredeep (green panels), and CTFB (orange panels), with the tectonic province indicated by the color of the subplot border.

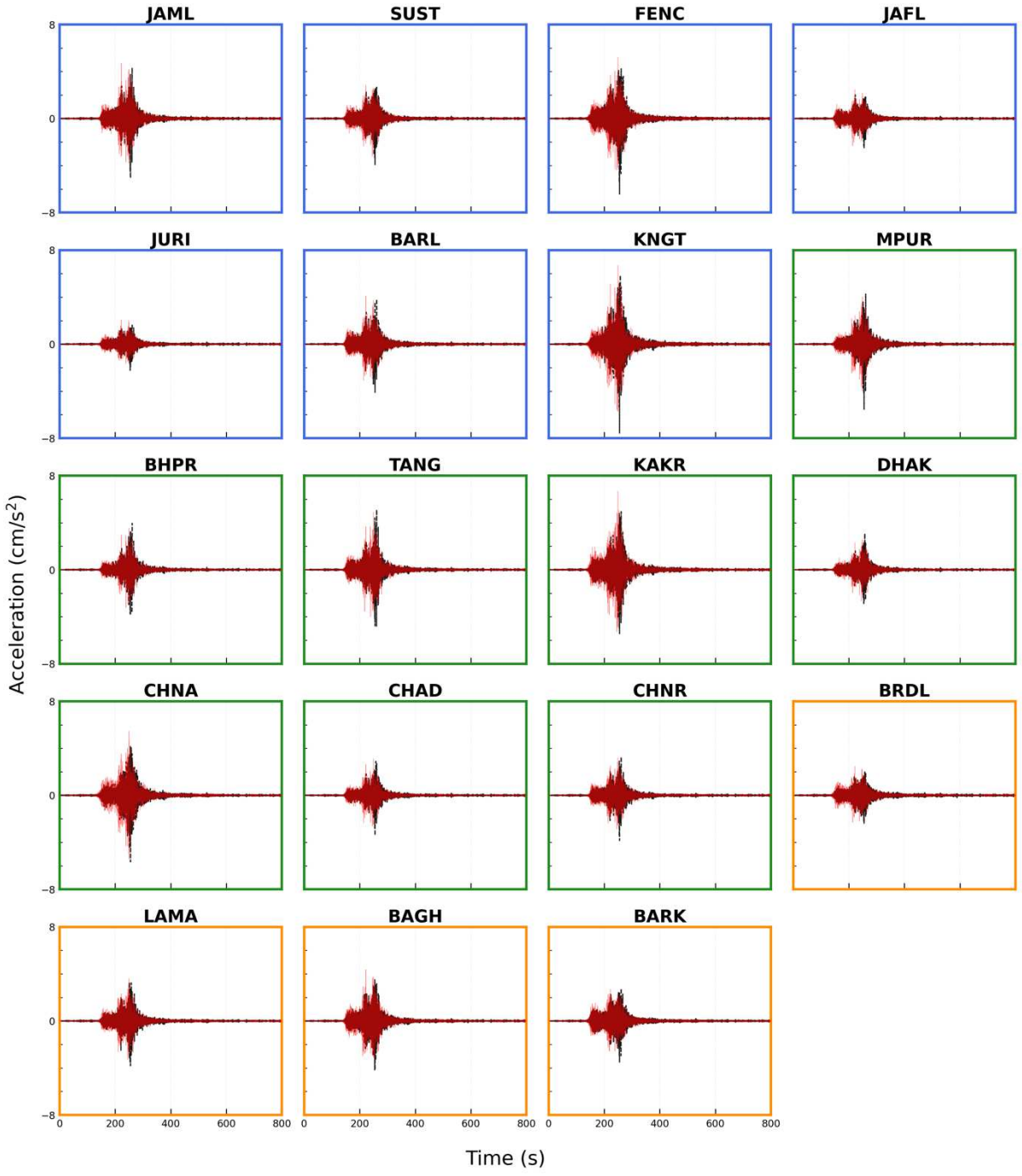


Figure 6. Synthetic accelerograms computed for the 19 seismic stations used in this study, showing PGA for both the M_W 6.7 (black color) and 7.3 events (red color) at each station. Stations are grouped according to their tectonic setting, namely the Surma Basin (blue panels),

Central Bengal Foredeep (green panels), and CTFB (orange panels), with the tectonic province indicated by the color of the subplot border.

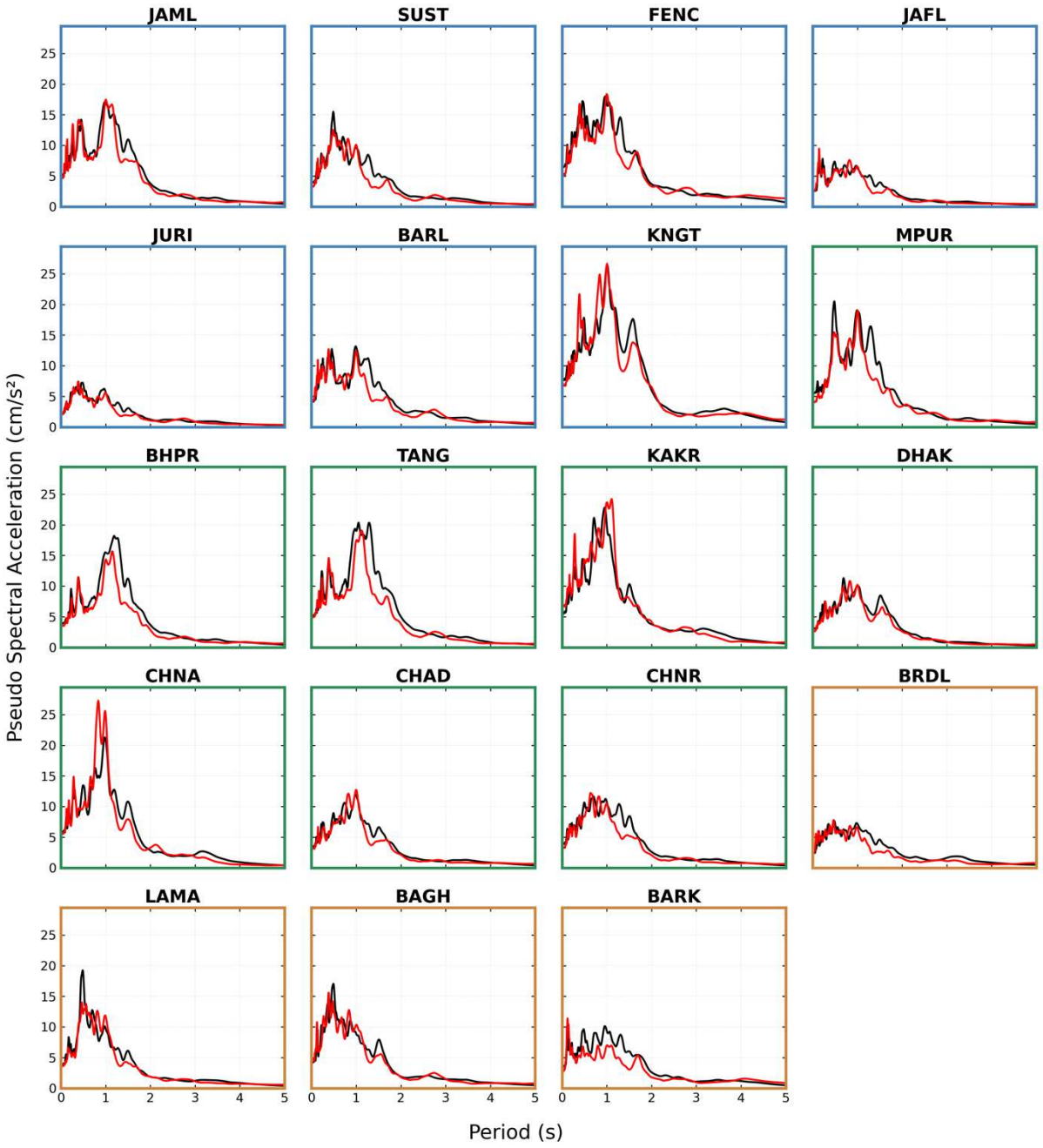


Figure 7. Pseudo-spectral acceleration (PSA) spectra computed for the 19 seismic stations used in this study, showing the 5%-damped response spectra for both the M_W 6.7 (black color) and M_W 7.3 (red color) subduction earthquake events at each station. Stations are grouped according to their tectonic setting, namely the Surma Basin (blue panels), Central Bengal Foredeep (green panels), and CTFB (orange panels), with the tectonic province indicated by the color of the subplot border.

Table 3. Seismic site classification based on soil properties (V_{S30} and SPT-N value).

Site Class	General Description	Vs30 (m/s)	SPT-N value
SA	Hard rock	>1500	
SB	Rock	760–1500	>50
SC	Very dense soil and soft rock	360–760	>15
SD	Stiff soil	180–360	<15
SE	Soft soil	<180	
SF	Soils requiring site-specific evaluation (e.g., liquefiable soils, highly organic soils, peat, sensitive clays, etc.)	—	

5. Results

5.1. Transfer Function

The vertically propagated 1D SH-wave transfer functions estimated for the 19 seismic stations using the synthetic ground motions generated from the two reference earthquakes (Mw 6.7 and Mw 7.3) are presented in Figure 5. The maximum transfer function amplitudes range from 4.37 at CHAD to 17.40 at CHNA. Among the Surma Basin stations, KNGT exhibits the highest amplification (13.49) with a dominant frequency of 0.97 Hz, whereas JURI shows the lowest amplification (4.55) and the highest dominant frequency (15.28 Hz). In the central Bengal Foredeep, CHNA records the largest amplification of all stations (17.40) at 3.17 Hz, followed by KAKR (13.51) and MPUR (10.24). In contrast, CHAD and CHNR exhibit relatively small amplification factors despite their different dominant frequencies. Within the CTFB, BARK (13.88) and BRDL (12.20) display relatively large amplification, whereas LAMA and BAGH show moderate values.

The observed differences in transfer function characteristics indicate that local site response is strongly influenced by local site conditions rather than by earthquake magnitude alone. The high amplification observed at CHNA, KAKR, KNGT, and BARK suggests the presence of strong impedance contrasts within the shallow sedimentary sequence, which enhance seismic-wave amplification. Conversely, stations such as CHAD, JURI, JAFL, and DHAK exhibit

comparatively low amplification, implying weaker impedance contrasts or more gradual increases in V_S with depth.

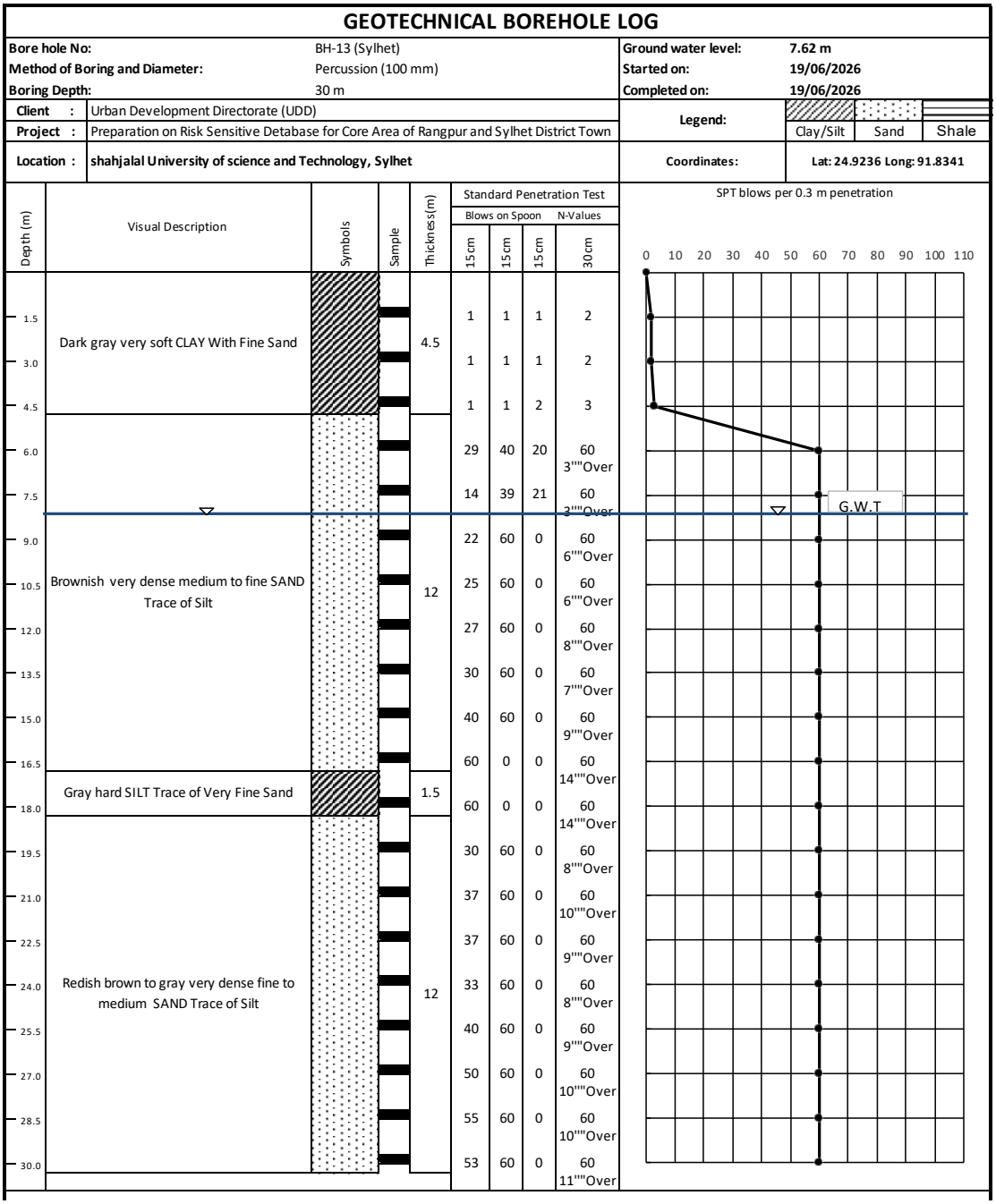


Figure 8. Example of a standard penetration test (SPT) borehole log for sub-soil investigation, conducted near station SUST at Sylhet City (Surma Basin), up to 30 m depth showing depth wise ST-N value from blow count and encountered lithology while boring.

Table 4. Comparison of seismic site classifications obtained from HVSR derived V_{S30} (Farazi et al., 2023), V_{S30} estimated using the Dhaka-specific SPT–V_S correlation proposed by Shehab

(2015), and site classes independently assigned from SPT-N values following the BNBC (2020) site classification scheme.

Station	Lat E	Long N	Vs Profile from HVSR		Mean SPT-N Value from Boring	VS-SPT-N Correlaiton of Dhaka Soil		Site Class from SPT-N according to BNBC (2020)
			Vs30 (m/s)	Site-Class from HVSR		Vs30 (m/s) from SPT-N	Site Class from SPT-N	
BAGH*	23.162001	92.192001	571.5	SC				
BARK	22.725599	92.375	591.9	SC	20.53	334.62	SD	SC
BARL*	24.691	92.185997	417.4	SC				
BHPR*	24.457001	89.875	432.3	SC				
BRDL	22.677999	91.642998	535.7	SC	12.77	474.85	SC	SD
CHAD	23.200001	90.983002	319	SD	9.88	248.12	SD	SD
CHNA	23.4904	91.008698	276.9	SD	12.63	271.11	SD	SD
CHNR*	24.1898	91.514999	391.2	SC				
DHAK	23.73	90.400002	239.4	SD	17.43	305.95	SD	SC
FENC	24.697001	91.936996	726.8	SC	20..33	366.39	SC	SC
JAFL	25.179001	92.018997	521.8	SC**	8.38	234.83	SD	SD
JAML	25.0005	91.237099	369.4	SC	9.62	246.31	SD	SD
JURI*	24.497999	92.135002	447	SC				
KAKR	24.070999	90.219002	406.6	SC**	14.8	200	SD	SD
KNGT*	25.01	92.253998	313.9	SD				
LAMA	21.775	92.199997	495.5	SC	50	530	SC	SC
MPUR*	24.604	90.029999	181.9	SD				
SUST	24.923	91.834	390.7	SC**	12.69	288.12	SD	SD
TANG	24.275999	89.921997	494.1	SC	16.18	265.84	SD	SC

*Site with only HVSR derived V_{S30} profile and site class.

** Site where HVSR derived site class matches none of the SPT-N value-based class criteria.

The dominant frequencies also vary substantially, from less than 1 Hz at BHPR and KNGT to more than 13 Hz at BRDL and 15 Hz at JURI. Lower dominant frequencies generally indicate thicker or lower-velocity sedimentary deposits, whereas higher frequencies are consistent with

relatively shallow impedance contrasts or stiffer near-surface materials. This broad frequency range demonstrates the pronounced lateral heterogeneity of near-surface geological conditions across Bangladesh and suggests that local site effects can differ considerably even between stations located within the same tectonic province.

5.2. Peak Ground acceleration (PGA)

The peak ground accelerations (PGAs) computed from the synthetic seismograms for the M_W 6.7 and M_W 7.3 earthquakes are presented in Figure 6. For the Mw 6.7 earthquake, the largest PGA is observed at KNGT (7.57 cm/s²), followed by FENC (6.43 cm/s²), CHNA (5.66 cm/s²), MPUR (5.54 cm/s²), and KAKR (5.45 cm/s²). In contrast, JURI (2.23 cm/s²) and BRDL (2.38 cm/s²) record the lowest PGAs. The spatial pattern for the Mw 7.3 event is broadly similar, although KAKR exhibits the highest PGA (6.70 cm/s²), closely followed by KNGT (6.71 cm/s²), CHNA (5.46 cm/s²), and FENC (5.20 cm/s²). Most stations show slightly lower PGAs for the M_W 7.3 event than for the M_W 6.7 event, while KAKR, BAGH, and BRDL display modest increases.

The regional distribution of PGA generally follows the transfer function characteristics, with stations exhibiting larger transfer function amplitudes also tending to produce stronger ground motions. However, the correspondence is not uniform. For example, BRDL shows one of the highest transfer function amplitudes but relatively low PGA, whereas CHNA and KNGT exhibit both high transfer function amplitudes and high PGAs. This difference reflects the fact that PGA depends not only on local amplification but also on the frequency content of the incoming wavefield.

Although stations within the same tectono-sedimentary region exhibit broadly comparable characteristics, noticeable variations remain within each region, emphasizing the influence of local subsurface conditions. The relatively high PGAs observed at several stations in the Surma Basin and the central Bengal Foredeep indicate that local site effects can substantially modify incoming seismic waves, whereas the generally moderate PGAs in the CTFB are consistent with the comparatively stiffer near-surface geological conditions. Even though not directly comparable, the spatial variability observed in this study is also broadly consistent with the regional pattern of seismic hazard shown in the BNBC (2020) seismic zonation map (Fig. 3), where stations located in Zones III and IV generally exhibit higher PGAs than those in Zone II, although local deviations caused by site effects are evident.

It should be noted that the simulated PGA values are considerably smaller than the design-level peak ground accelerations specified in BNBC (2020), which range from 0.12 g to 0.36 g across the four seismic zones. This difference is expected because the synthetic seismograms were generated using reference motions recorded at the hard-rock station SHL from earthquakes located approximately 1,162 km from Bangladesh. Such far-field ground motions undergo substantial attenuation before reaching the study area and therefore cannot be expected to reproduce code-level design accelerations associated with scenario earthquakes closer to Bangladesh. Nevertheless, the present simulations remain valuable for seismic hazard assessment because all stations were subjected to the same reference input motion, allowing differences in the resulting PGAs to be attributed primarily to local site response. Consequently, the relative spatial variation of PGA provides useful insight into the influence of near-surface geological conditions on earthquake ground motions and complements the regional seismic hazard pattern represented by the BNBC (2020) zonation map (Fig. 3).

5.3. Spectral Acceleration

The 5%-damped pseudo-spectral acceleration (PSA) response spectra for the M_W 6.7 and Mw 7.3 synthetic earthquakes are presented in Figure 7. The corresponding spatial distribution of the average peak spectral period derived from the two earthquakes is shown in Figure 9. Unlike PGA, which represents the maximum ground acceleration, PSA identifies the spectral period at which seismic waves are preferentially amplified and is therefore particularly relevant for evaluating the dynamic response of structures.

The simulated peak PSA values exhibit considerable spatial variability, ranging from 7.25 to 26.58 cm/s² for the Mw 6.7 earthquake and from 7.44 to 27.39 cm/s² for the Mw 7.3 earthquake. KNGT consistently records the largest spectral accelerations for both events (26.58 and 26.76 cm/s²), followed by CHNA (21.39 and 27.39 cm/s²), KAKR (22.95 and 24.35 cm/s²), MPUR (20.55 and 19.10 cm/s²), and TANG (20.35 and 19.13 cm/s²). In contrast, JAFL, JURI, and BRDL exhibit the lowest spectral accelerations. The overall distribution closely resembles the transfer function characteristics, indicating that stronger site amplification generally produces larger spectral demands on structures.

A notable feature of the response spectra is the concentration of peak spectral periods near 1 s at many stations. KNGT, JAML, FENC, TANG, KAKR, CHNA, and BHPR all exhibit dominant periods between approximately 0.95 and 1.20 s, while DHAK and CHNR show

intermediate periods of about 0.64–0.84 s. Conversely, stations such as BARK and JAFL display much shorter dominant periods (0.12–0.22 s), reflecting comparatively stiffer near-surface conditions. The spatial distribution of average peak spectral period (Fig. 10) further demonstrates that periods close to 1 s are widespread across the Surma Basin and the central Bengal Foredeep. This result suggests that distant large-magnitude earthquakes may produce amplification in longer periods in regions underlain by thick sedimentary deposits. On the other hands, shorter periods are more common within parts of the CTFB, reflecting the comparatively older and stiffer geological units have come closer to the surface probably due to upliftment of the fold belt (Farazi et al., 2023). Overall, the results underscore that, even under the same far-field excitation, the spectral characteristics of ground motion vary substantially across Bangladesh owing to differences in local site conditions (Khan et al., 2025).

5.4. Seismic Site Classes

The seismic site classifications derived from the HVSR inversion-based V_{S30} profiles, the V_{S30} estimated using the Dhaka soil SPT–V_S empirical correlations, and the SPT-N based BNBC (2020) classification are summarized in Table 4. The spatial distribution of the final site classifications adopted in this study, based on the HVSR derived V_{S30}, is presented in Figure 10. Since the transfer function and pseudo-spectral acceleration analyses were computed using the HVSR inversion velocity profiles, the corresponding HVSR derived site classes are considered the representative classifications, whereas the SPT based classifications are used for independent validation.

The HVSR derived V_{S30} values range from 181.9 to 726.8 m/s, corresponding to two BNBC (2020) site classes: SC and SD. Twelve of the nineteen stations are classified as SC, while the remaining seven stations are classified as SD. Regionally, most stations in the Surma Basin and the CTFB are classified as SC, reflecting relatively higher near-surface V_S, whereas SD sites are predominantly distributed within the central Bengal Foredeep, including MPUR, CHAD, CHNA, DHAK, and KNGT. Herein, the predominance of site class SC may also reflect the siting strategy of permanent seismic stations, which are typically installed on relatively competent ground and stable concrete foundations to minimize environmental noise and ensure reliable seismic recordings.

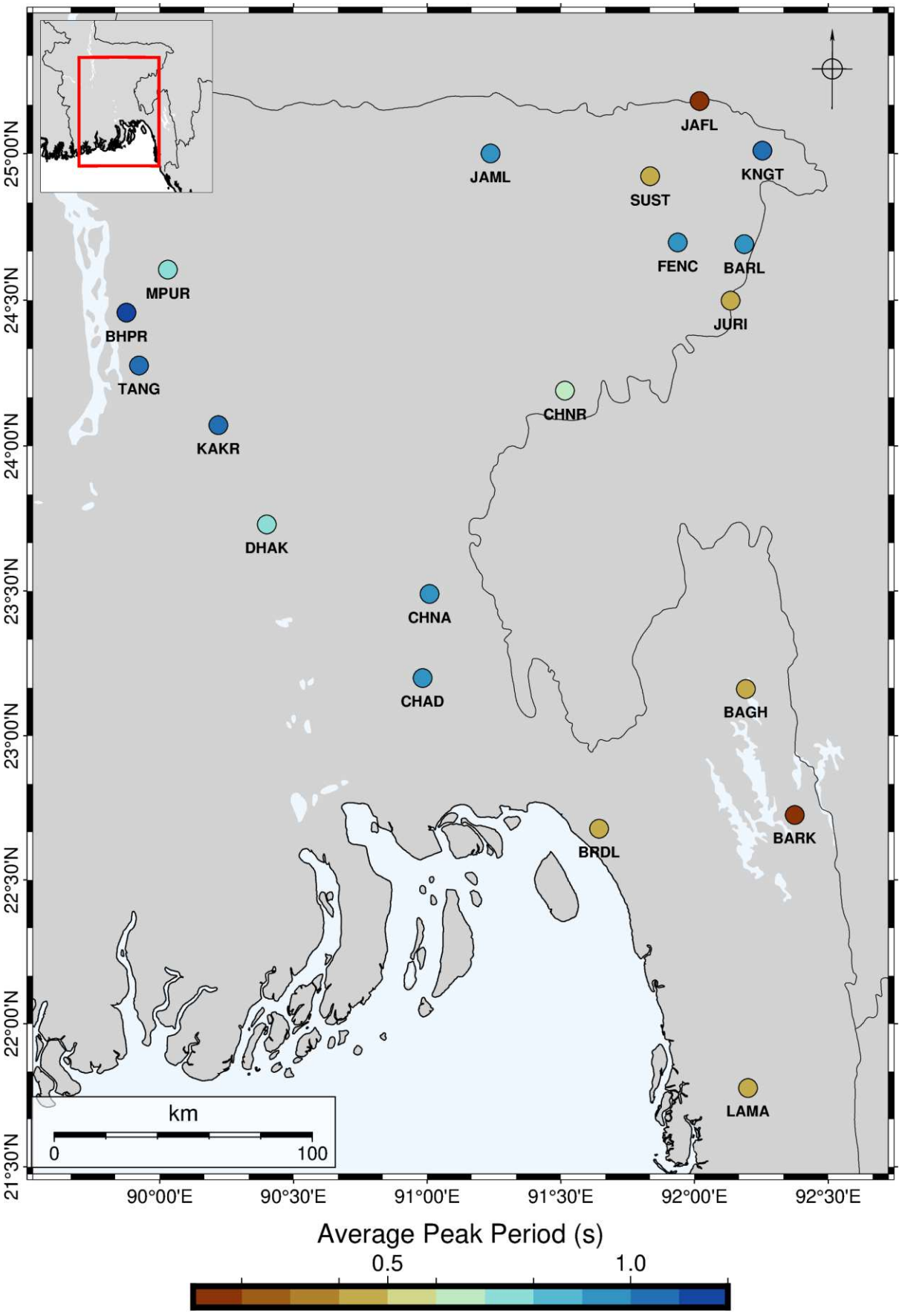
Among the twelve stations with borehole investigations, the site classifications derived from the Dhaka soil SPT–V_S correlations agree with the HVSR-derived classifications at eight

582 stations (67%), including BARK, BRDL, CHAD, CHNA, DHAK, FENC, LAMA, and TANG.
583 The remaining four stations (JAFL, KAKR, SUST, and JAML) are classified as SC using the
584 HVSR-derived V_{S30} but as SD using the SPT-based V_{S30} estimates. Similarly, comparison with
585 the BNBC (2020) SPT-N classification also shows agreement at eight of the twelve stations,
586 while discrepancies are observed at BRDL, DHAK, JAFL, and TANG. Overall, both validation
587 approaches indicate a generally good correspondence with the HVSR-derived classifications
588 despite a limited number of mismatches.

589 The differences between the three classification methods are expected because they are based
590 on fundamentally different datasets and assumptions. The HVSR derived V_{S30} values are
591 obtained from inversion of ambient-noise measurements and represent continuous V_S profiles
592 constrained by the observed site resonance, whereas the SPT-based classifications are inferred
593 from empirical relationships developed for Dhaka soils or from average penetration resistance
594 within the upper 30 m. The application of the Dhaka-specific SPT–Vs correlations to other
595 geological environments across Bangladesh may therefore introduce additional uncertainty,
596 particularly in the Surma Basin and the CTFB, where lithological conditions differ from those
597 of the Dhaka area.

598 Although some discrepancies exist, the overall agreement between the HVSR derived and SPT
599 based classifications supports the reliability of the inverted V_S models. Therefore, the HVSR
600 derived site classes provide a reasonable basis for interpreting the transfer functions and
601 pseudo-spectral accelerations presented in the preceding sections, while offering seismic site
602 characterization at locations where borehole information is unavailable, which has been done
603 by many (Ghione et al., 2023; Lontsi et al., 2026).

604


JAFL
JAML
KNGT
SUST
FENC
BARL
JURI
MPUR
BHPR
TANG
CHNR
KAKR
DHAK
CHNA
CHAD
BAGH
BRDL
BARK
LAMA
25°00'N
24°30'N
24°00'N
23°30'N
23°00'N
22°30'N
22°00'N
21°30'N
90°00'E
90°30'E
91°00'E
91°30'E
92°00'E
92°30'E
km
0
100
Average Peak Period (s)
0.5
1.0

605

Figure 9. Spatial distribution of the average peak period across the seismic stations in Bangladesh. Colored circles denote seismic stations and are shaded according to the average peak period (s), calculated by averaging the peak periods obtained from the pseudo-spectral acceleration response to the M_W 6.7 and M_W 7.3 input earthquake motions. The horizontal color bar indicates the corresponding average peak-period values. Station codes are shown below each circle. The inset map depicts the location of the study area within Bangladesh, with the red rectangle indicating the area covered by the main map.

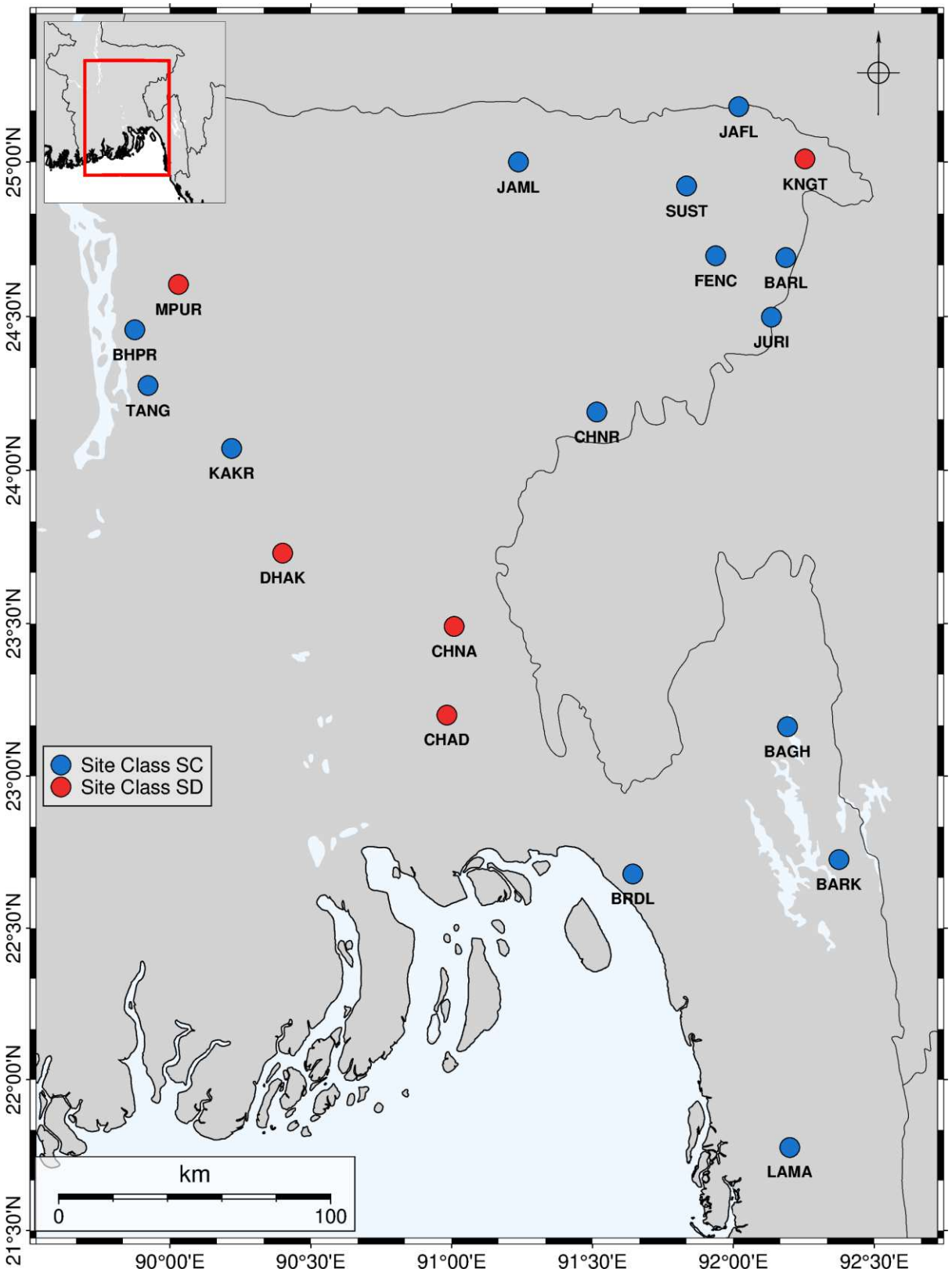


Figure 10. Spatial distribution of the seismic site classes at the seismic station locations across Bangladesh, estimated from the V_{S30} values derived from the V_S profiles of Farazi et al. (2023). Station codes are shown below each circle for identification. The inset map depicts the location

of the study area within Bangladesh, with the red rectangle indicating the area covered by the main map.

6. Discussion

The primary motivation of this study was to evaluate the response of the thick sedimentary deposits of the Bengal Basin to far-field earthquakes, inspired by the widespread long-period shaking observed in the Bangkok Basin during the March 2025 M_W 7.7 Myanmar supershear earthquake, which caused severe oscillation of high-rise buildings and the collapse of one high-rise structure (Ornthammarath et al., 2025; Pananont et al., 2026). Therefore, the objective of the study was not to investigate amplification factors but to investigate the potential of far-field earthquake amplification and its dominant periods in case of the thick soft sedimentary Bengal Basin in Bangladesh. Although the simulated earthquakes considered here produce relatively small PGAs because of the large source-to-site distance (~1,162 km), the transfer functions and response spectra consistently demonstrate that far-field seismic waves can still be significantly modified by local geological conditions. Because both reference earthquakes are distant and differ in magnitude and source characteristics, direct comparison of amplification amplitudes is of limited significance. Nevertheless, both simulations consistently indicate similar dominant spectral periods at individual stations, suggesting that these periods are controlled primarily by local geological conditions rather than by the input motion itself.

The combined analyses of transfer function, PGA, PSA, and seismic site classification indicate that engineering bedrock depth exerts a first-order control on long-period site response. Stations underlain by thicker sedimentary sequences generally exhibit lower transfer-function peak frequencies and larger long-period spectral accelerations, whereas stations with shallower engineering bedrock tend to amplify shorter-period motions. Many stations in the Surma Basin and the central Bengal Foredeep exhibiting dominant periods close to 1.0 s and even beyond. This behavior reflects the increasing travel time of seismic waves through low-velocity sediments and the stronger impedance contrast between engineering bedrock and the overlying deposits. Figure 11 demonstrates this relationship by showing a systematic increase in dominant spectral period as a function of engineering bedrock depth,

Comparison with the BNBC (2020) design spectral period ranges further highlights the importance of deep sedimentary structure (Fig. 11). Although the HVSR-derived seismic site classifications show good agreement with those obtained from the Dhaka soil SPT–Vs

649 correlations and the BNBC (2020) SPT-N classification, the observed peak spectral periods at
650 many SC and SD sites extend beyond the period ranges represented by the BNBC design
651 spectra. This suggests that even though the current BNBC (2020) classification may adequately
652 characterizes the stiffness of the uppermost 30 m through V_{S30} (or equivalent SPT criteria), but
653 does not explicitly account for the influence of engineering bedrock depth on long-period
654 amplification. Consequently, sites with similar V_{S30} may exhibit markedly different spectral
655 characteristics because of differences in deep sedimentary structure.

656 These observations are consistent with recent site-response studies in Bangladesh. Using
657 nonlinear one-dimensional site response analysis for Chattogram, Zaman et al. (2026) showed
658 that the BNBC (2020) design spectrum generally provides reasonable estimates of PGA but
659 may be non-conservative at medium-to-long periods, emphasizing the need for site-specific
660 response analyses. Similarly, Rahman et al. (2021) demonstrated that the thick, soft sediments
661 beneath Dhaka preferentially de-amplify short-period motions while amplifying long-period
662 ground motions, explaining the relatively limited damage to low-rise buildings during
663 historical distant earthquakes and the increasing vulnerability of modern high-rise structures.
664 The predominant spectral periods of approximately 0.8–1.0 s obtained for several stations in
665 the present study are also consistent with the site response reported for Dhaka by Farazi et al.
666 (2023), further supporting the role of deep sedimentary deposits in controlling long-period
667 amplification across the Bengal Basin. These findings suggest that the deep soft sediments of
668 the Bengal Basin have the potential to amplify long-period ground motions from far-field
669 earthquakes and should therefore be considered in future seismic hazard assessments for
670 Bangladesh.

671 The reliability of the present analyses is supported by the generally good agreement between
672 the HVSR derived site classifications and those independently obtained from borehole SPT
673 data (Table 4). Moreover, the systematic relationship between engineering bedrock depth and
674 dominant spectral period provides additional confidence in the physical realism of the velocity
675 models used in this study.

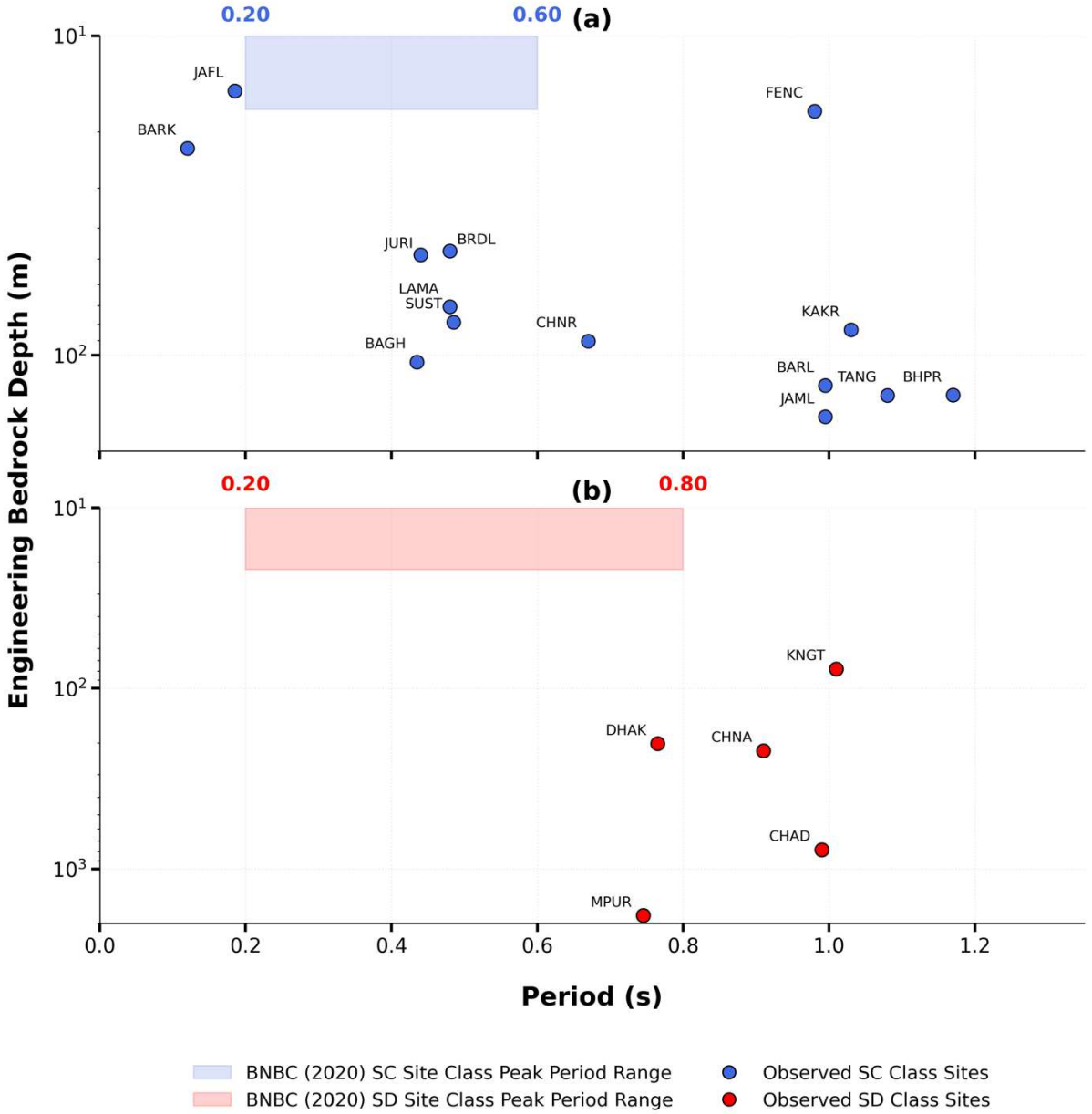


Figure 11. Comparison of the BNBC (2020) design-spectrum peak-period ranges for (a) Site Class SC and (b) Site Class SD with the average peak periods of the computed spectral acceleration from the M_W 6.7 and M_W 7.3 scenario events at individual seismic station. Peak periods are plotted as a function of engineering bedrock depth derived from the HVSR V_S models of Farazi et al. (2023).

Overall, this study demonstrates that seismic hazard in Bangladesh is governed not only by near-surface soil stiffness but also by the thickness of sedimentary deposits and the depth to engineering bedrock, providing a more realistic assessment of long-period ground motion in the Bengal Basin. Such considerations are particularly important for the seismic design and performance assessment of medium- and high-rise buildings, whose natural periods may

coincide with the amplified periods identified in this study during future large-magnitude far-field earthquakes. The findings further suggest that future revisions of the BNBC (2020) should explicitly consider the influence of deep sedimentary structure and engineering bedrock depth on long-period ground motion, in addition to the conventional V_{S30} based site classification. Moreover, while probabilistic seismic hazard assessment remains essential, analyses of observed strong-motion records are equally important for capturing the complex long-period response of exceptionally thick sedimentary basins such as the Bengal Basin.

Several limitations of this study should be acknowledged. The analyses are based on two scenario-based far-field earthquakes referenced to a single hard-rock station and employ one-dimensional linear elastic site response modeling through horizontally layered media. Consequently, the simulated ground motions represent regional response trends rather than project-specific design demands and should not be interpreted as design-level ground motions. The adopted methodology is appropriate for far-field, low-strain conditions but cannot capture nonlinear soil behavior, multidimensional basin effects (e.g., basin-edge effects, surface-wave generation, and seismic energy trapping), or complex source characteristics such as finite-fault rupture directivity and path-dependent attenuation. Furthermore, because the input motions were not selected or spectrum-matched following standard design procedures (e.g., NEHRP), the results should be regarded as preliminary and interpreted primarily in terms of dominant spectral period and long-period site response rather than absolute amplification levels.

Therefore, future research may expand incorporating a broader suite of representative regional and near-fault earthquake scenarios to encompass a wider range of frequency contents and ground motion amplitudes. Executing nonlinear or equivalent-linear site response analyses will better model high soil strain levels and potential cyclic degradation. Crucially, deploying 2D or 3D basin models is necessary to capture complex lateral wave propagation, basin-edge induced waves, and spatial resonance effects. Future efforts should also specifically examine near-fault forward directivity effects and directional resonance phenomena, which can drastically alter structural demands over localized areas. Despite its preliminary nature, this study may serve as a vital motivator for policymakers, urban planners, and structural engineers to explicitly account for deep soil amplification effects in thick sedimentary basins like the Bengal Basin, providing a foundational step toward earthquake resilience in Bangladesh.

7. Conclusions

This study presents the first regional-scale, simulation-based assessment of 1D linear seismic site response across the Bengal Basin, Bangladesh, using deep V_S profiles derived from HVSR inversion and two simulated far-field earthquake ground motions. Transfer functions, peak ground accelerations (PGAs), pseudo-spectral accelerations, and seismic site classifications were evaluated for 19 seismic stations representing the Surma Basin, the central Bengal Foredeep, and the Chittagong-Tripura Fold Belt (CTFB). Rather than quantifying absolute amplification levels, this study focuses on the dominant spectral response of the deep sedimentary Bengal Basin to far-field earthquake ground motions. The results demonstrate spatial variability in site response. Stations underlain by thicker sedimentary sequences and deeper engineering bedrock generally exhibit lower transfer-function peak frequencies and longer dominant spectral periods than those with shallower engineering bedrock. Consequently, the peak period of the elastic response spectrum increases with engineering bedrock depth, with many stations in the Surma Basin and the central Bengal Foredeep exhibiting dominant spectral periods close to 1 s. These periods coincide with the natural vibration periods of medium- to high-rise buildings, indicating a potential for structural resonance during future large-magnitude far-field earthquakes. In contrast, the comparatively shallower engineering bedrock and tectonically uplifted geology of the CTFB produce shorter dominant spectral periods, suggesting a relatively greater resonance potential for low-rise structures. Although the simulated earthquakes produced relatively low PGAs because of the large source-to-site distance, they demonstrate that deep sedimentary deposits can substantially modify and lengthen the period content of incoming seismic waves. The HVSR-derived V_{S30} based seismic site classifications show generally good agreement with those independently obtained from SPT borehole data, with all stations classified as either site class SC or SD according to BNBC (2020), supporting the reliability of the velocity models used for regional site-response analysis. The findings of this communication suggest that the deep soft sediments of the Bengal Basin have the potential to amplify long-period ground motions from far-field earthquakes. Accordingly, future revisions of the BNBC (2020) should consider engineering bedrock depth and deep sedimentary effects, in addition to the conventional V_{S30} based approach, to improve seismic hazard assessment and earthquake-resistant design in Bangladesh.

While the present study is bounded by a 1D linear elastic framework and specific far-field scenario motions, leaving the investigation of nonlinear soil effects, 3D basin geometry, and

scaled ground motion suites to future research, it establishes an important baseline for understanding regional period-dependent amplification characteristics across the Bengal Basin. Ultimately, the framework and basin-scale trends identified herein serves a preliminary role to motivate and assist policymakers, structural engineers, and urban planners in mitigating structural resonance risks and enhancing long-term earthquake preparedness and structural resilience in Bangladesh.

References

Aitchison, J. C., Ao, A., Bhowmik, S., Clarke, G. L., Ireland, T. R., Kachovich, S., Lokho, K., Stojanovic, D., Roeder, T., Truscott, N., Zhen, Y., & Zhou, R. (2019). Tectonic Evolution of the Western Margin of the Burma Microplate Based on New Fossil and Radiometric Age Constraints. *Tectonics*, *38*(5), 1718–1741. https://doi.org/10.1029/2018TC005049

Alam, M., Alam, M. M., Curray, J. R., Chowdhury, M. L. R., & Gani, M. R. (2003). An overview of the sedimentary geology of the Bengal Basin in relation to the regional tectonic framework and basin-fill history. *Sedimentary Geology*, *155*(3–4), 179–208. https://doi.org/10.1016/S0037-0738(02)00180-X

Ambraseys, N. N., & Douglas, J. (2004). Magnitude calibration of north Indian earthquakes. *Geophysical Journal International*, *159*(1), 165–206. https://doi.org/10.1111/J.1365-246X.2004.02323.X

Ansary, M. A., & Arefin, M. R. (2019). Assessment of predominant frequencies in Dhaka city, Bangladesh using ambient vibration. *Asian Journal of Civil Engineering 2019 21:1*, *21*(1), 91–104. https://doi.org/10.1007/S42107-019-00194-2

Ansary, M. A., Noor, M. A., & Rashid, M. A. (2004). Site amplification characteristics of Dhaka city. *Journal of Civil Engineering (IEB)*, *32*(1), 1–16.

Bard, P.-Y., & Bouchon, M. (1985). The two-dimensional resonance of sediment-filled valleys. *Bulletin of the Seismological Society of America*, *75*(2), 519–541. https://doi.org/10.1785/bssa0750020519

Bard, P. Y., & Gariel, J. C. (1986). The seismic response of two-dimensional sedimentary deposits with large vertical velocity gradients. *Bulletin of the Seismological Society of*

America, *76*(2), 343–366. https://doi.org/10.1785/BSSA0760020343

Berge-Thierry, C., Bernard, P., & Herrero, A. (2001). Simulating strong ground motion with the “k-2” kinematic source model: An application to the seismic hazard in the Erzincan basin, Turkey. *Journal of Seismology*, *5*(1), 85–101. https://doi.org/10.1023/A:1009829129344/METRICS

Bilham, R. (2004). Earthquakes in India and the Himalaya: Tectonics, geodesy and history. *Annals of Geophysics*, *47*(2–3), 839–858. https://doi.org/10.4401/ag-3338

Bilham, R., & Hough, S. (2006). Future Earthquakes on the Indian Subcontinent: Inevitable Hazard, Preventable Risk. *South Asian Journal*, *12*, 1–9.

BNBC. (2020). *Bangladesh National Building Code (BNBC). Housing and Building Research Institute, Ministry of Housing and Public Works, Government of the People’s Republic of Bangladesh*. http://hbri.gov.bd/pages/static-pages/6922e02d933eb65569e25da9

Borcherdt, R. D. (1994). 1. Estimates of Site-Dependent Response Spectra for Design (Methodology and Justification). *Earthquake Spectra*, *10*(4), 617–653. https://doi.org/10.1193/1.1585791

Bürgi, P., Hubbard, J., Akhter, S. H., & Peterson, D. E. (2021). Geometry of the Décollement Below Eastern Bangladesh and Implications for Seismic Hazard. *Journal of Geophysical Research: Solid Earth*, *126*(8), e2020JB021519. https://doi.org/10.1029/2020JB021519

Chopra, A. K. (1995). *Dynamics of Structures: Theory and Applications to Earthquake Engineering* (B. Stenquist & K. Scherwatzky (eds.); 1st ed.). Prentice Hall.

Chowdhury, I. N., Cabas, A., Kaklamanos, J., Kottke, A., & Gregor, N. (2024). Implications of input ground-motion selection techniques on site response analyses for different tectonic settings. *Earthquake Spectra*, *40*(2), 1521–1551. https://doi.org/10.1177/87552930241230917;ISSUE:ISSUE:DOI

Cruz-Atienza, V. M., Tago, J., Sanabria-Gómez, J. D., Chaljub, E., Etienne, V., Virieux, J., & Quintanar, L. (2016). Long Duration of Ground Motion in the Paradigmatic Valley of Mexico. *Scientific Reports 2016 6:1*, *6*(1), 38807-. https://doi.org/10.1038/SREP38807

Farazi, A. H., Hossain, M. S., Ito, Y., Piña-Flores, J., Kamal, A. S. M. M., & Rahman, M. Z. (2023). Shear wave velocity estimation in the Bengal Basin, Bangladesh by HVSR analysis: implications for engineering bedrock depth. *Journal of Applied Geophysics*,

211, 104967. https://doi.org/10.1016/J.JAPPGEO.2023.104967

Furumura, T., & Kennett, B. L. N. (2019). The Significance of Long-Period Ground Motion at Regional to Teleseismic Distances From the 610-km Deep Mw 8.3 Sea of Okhotsk Earthquake of 24 May 2013. *Journal of Geophysical Research: Solid Earth*, *124*(8), 9075–9094. https://doi.org/10.1029/2019JB018147

Gallipoli, M. R., Mucciarelli, M., Castro, R. R., Monachesi, G., & Contri, P. (2004). Structure, soil–structure response and effects of damage based on observations of horizontal-to-vertical spectral ratios of microtremors. *Soil Dynamics and Earthquake Engineering*, *24*(6), 487–495. https://doi.org/10.1016/J.SOILDYN.2003.11.009

Ghione, F., Köhler, A., Dichiarante, A. M., Aarnes, I., & Oye, V. (2023). Vs30 and depth to bedrock estimates from integrating HVSR measurements and geology-slope approach in the Oslo area, Norway. *Frontiers in Earth Science*, *11*, 1242679. https://doi.org/10.3389/FEART.2023.1242679/TEXT

Goodbred, S. L., Kuehl, S. A., Steckler, M. S., & Sarker, M. H. (2003). Controls on facies distribution and stratigraphic preservation in the Ganges-Brahmaputra delta sequence. *Sedimentary Geology*, *155*(3–4), 301–316. https://doi.org/10.1016/S0037-0738(02)00184-7

Hossain, M. S., Kamal, A. S. M. M., Rahman, M. Z., Farazi, A. H., Mondal, D. R., Mahmud, T., & Ferdous, N. (2020). Assessment of soil liquefaction potential: a case study for Moulvibazar town, Sylhet, Bangladesh. *SN Applied Sciences*, *2*(4). https://doi.org/10.1007/s42452-020-2582-x

Hossain, M. S., Numada, M., Mitu, M., Timsina, K., Krisna, C., Rahman, M. Z., Kamal, A. S. M. M., & Meguro, K. (2023). Simplified engineering geomorphic unit-based seismic site characterization of the detailed area plan of Dhaka city, Bangladesh. *Scientific Reports*, *13*(1), 1–14. https://doi.org/10.1038/S41598-023-37628-6;SUBJMETA=166,4111,639,704,986;KWRD=CIVIL+ENGINEERING,NATURAL+HAZARDS

Janusz, P., Panzera, F., Bergamo, P., Perron, V., & Fäh, D. (2025). Mapping site amplification with the dense recording of ambient vibration for the city of Lucerne (Switzerland): comparison between two approaches. *Bulletin of Earthquake Engineering 2025 23:4*, *23*(4), 1431–1462. https://doi.org/10.1007/S10518-024-02091-9

Johnson, S. Y., & Alam, A. M. N. (1991). Sedimentation and tectonics of the Sylhet trough, Bangladesh. *Geological Society of America Bulletin*, *103*(11), 1513. https://doi.org/10.1130/0016-7606(1991)103<1513:SATOTS>2.3.CO;2

Kaklamanos, J., Baise, L. G., Thompson, E. M., & Dorfmann, L. (2015). Comparison of 1D linear, equivalent-linear, and nonlinear site response models at six KiK-net validation sites. *Soil Dynamics and Earthquake Engineering*, *69*, 207–219. https://doi.org/10.1016/J.SOILDYN.2014.10.016

Kamal, A. S. M. M., Mitu, M., Hossain, M. S., Rahman, M. M., & Rahman, M. Z. (2021). Seismic Hazard Analysis for the South-Central Coastal Region of Bangladesh Considering the Worst-Case Scenario. *Pure and Applied Geophysics*, *178*(8), 2821–2838. https://doi.org/10.1007/S00024-021-02770-7/METRICS

Kennett, B. L. N., & Kerry, N. J. (1979). Seismic waves in a stratified half space. *Geophysical Journal International*, *57*(3), 557–583. https://doi.org/10.1111/J.1365-246X.1979.TB06779.X

Khan, A. A., & Chouhan, R. K. S. (1996). The crustal dynamics and the tectonic trends in the Bengal Basin. *Journal of Geodynamics*, *22*(3–4), 267–286. https://doi.org/10.1016/0264-3707(96)00022-1

Khan, M. M. H., Sisi, A. A., Hobiger, M., Rahman, M. A., & Jabeen, S. (2025). Local Peak Ground Acceleration from Probabilistic Seismic Hazard Assessment: Methodology and Application for Engineering Design in Bangladesh. *Asian Journal of Engineering Geology*, *2*(Sp Issue), 95–96. https://doi.org/10.64862/AJEG.2025.2SP.44.148

Kramer, S. L., & Stewart, J. P. (2024). *Geotechnical Earthquake Engineering*. CRC Press. https://doi.org/10.1201/9781003512011

Lizundia, B., Davidson, R. A., Hashash, Y. M. A., & Olshansky, R. (2017). Overview of the 2015 Gorkha, Nepal, Earthquake and the Earthquake Spectra Special Issue. *Earthquake Spectra*, *33*(1S), 1–20. https://doi.org/10.1193/120817eqs252m

Lontsi, A. M., Tchapleu, J. F. T., Tokam, A. P. K., Ndiparray, J. T., Ndibi, D. D. E., Beteh, S., Jimmesiy, A. W., & Tabod, T. C. (2026). Seismic site characterization and classification in Cameroon using full microtremor horizontal-to-vertical spectral ratio analysis and inversion. *Soil Dynamics and Earthquake Engineering*, *203*, 110039. https://doi.org/10.1016/J.SOILDYN.2025.110039

875 Manea, E. F., Cioflan, C. O., Coman, A., Michel, C., Poggi, V., & Fäh, D. (2020). Estimating
876 Geophysical Bedrock Depth Using Single Station Analysis and Geophysical Data in the
877 Extra-Carpathian Area of Romania. *Pure and Applied Geophysics*, *177*(10), 4829–4844.
878 https://doi.org/10.1007/s00024-020-02548-3

879 Maurin, T., & Rangin, C. (2009). Structure and kinematics of the Indo-Burmese Wedge:
880 Recent and fast growth of the outer wedge. *Tectonics*, *28*(2).
881 https://doi.org/10.1029/2008TC002276

882 Mitra, S., Priestley, K. F., Borah, K., & Gaur, V. K. (2018). Crustal Structure and Evolution
883 of the Eastern Himalayan Plate Boundary System, Northeast India. *Journal of*
884 *Geophysical Research: Solid Earth*, *123*(1), 621–640.
885 https://doi.org/10.1002/2017JB014714

886 Mitra, S., Priestley, K., Gaur, V. K., Rai, S. S., & Haines, J. (2006). Variation of Rayleigh
887 wave group velocity dispersion and seismic heterogeneity of the Indian crust and
888 uppermost mantle. *Geophysical Journal International*, *164*(1), 88–98.
889 https://doi.org/10.1111/j.1365-246X.2005.02837.x

890 Mitu, M., Rahman, M. Z., Kamal, A. S. M. M., & Hossain, M. S. (2025). Nonlinear Site
891 Response of Dhaka Soil Using Local Earthquake Records. *Geotechnical and Geological*
892 *Engineering*, *43*(7), 1–20. https://doi.org/10.1007/S10706-025-03322-9/METRICS

893 Molnar, P., & Tapponnier, P. (1975). Cenozoic tectonics of Asia: Effects of a continental
894 collision. In *Science* (Vol. 189, Issue 4201, pp. 419–426).
895 https://doi.org/10.1126/science.189.4201.419

896 Molnar, S., Cassidy, J. F., Castellaro, S., Cornou, C., Crow, H., Hunter, J. A., Matsushima,
897 S., Sánchez-Sesma, F. J., & Yong, A. (2018). Application of Microtremor Horizontal-to-
898 Vertical Spectral Ratio (MHVSR) Analysis for Site Characterization: State of the Art.
899 *Surveys in Geophysics*, *39*(4), 613–631. https://doi.org/10.1007/s10712-018-9464-4

900 Molnar, S., Sirohey, A., Assaf, J., Bard, P.-Y., Castellaro, S., Cornou, C., Cox, B., Guillier,
901 B., Hassani, B., Kawase, H., Matsushima, S., Sánchez-Sesma, F. J., & Yong, A. (2022).
902 A review of the microtremor horizontal-to-vertical spectral ratio (MHVSR) method.
903 *Journal of Seismology*, *26*(4), 653–685. https://doi.org/10.1007/s10950-021-10062-9

904 Morino, M., Maksud Kamal, A. S. M., Muslim, D., Ekram Ali, R. M., Kamal, M. A., Zillur
905 Rahman, M., & Kaneko, F. (2011). Seismic event of the Dauki Fault in 16th century

906 confirmed by trench investigation at Gabrakhari Village, Haluaghat, Mymensingh,
907 Bangladesh. *Journal of Asian Earth Sciences*, *42*(3), 492–498.
908 https://doi.org/10.1016/j.jseaes.2011.05.002

909 Najman, Y., Bickle, M., BouDagher-Fadel, M., Carter, A., Garzanti, E., Paul, M., Wijbrans,
910 J., Willett, E., Oliver, G., Parrish, R., Akhter, S. H., Allen, R., Ando, S., Chisty, E.,
911 Reisberg, L., & Vezzoli, G. (2008). The Paleogene record of Himalayan erosion: Bengal
912 Basin, Bangladesh. *Earth and Planetary Science Letters*, *273*(1–2), 1–14.
913 https://doi.org/10.1016/J.EPSL.2008.04.028

914 Oldham, R. (1899). *Report of the great earthquake of 12th June, 1897,*. Office of the
915 Geological Survey.

916 Ordaz, M., & Montoya, C. (2000). *DEGTRA A4* (5.4.0). Instituto de Ingenieria, UNAM.

917 Ornthammarath, T., Warnitchai, P., Maruyama, Y., Pornsopin, P., & Yamazaki, F. (2025).
918 Far-field ground motion characteristics of the Bangkok Basin, Thailand, in the 2025 Mw
919 7.7 Mandalay earthquake: initial insights. *Bulletin of Earthquake Engineering 2025*
920 *23:15*, *23*(15), 6577–6602. https://doi.org/10.1007/S10518-025-02295-7

921 Pananont, P., Pholsonda, P., Pornsopin, P., Furlong, K., Hayashi, K., Muangnoi, S., &
922 Prasertwongphilai, K. (2026). Observed H/V Responses Across Thailand from the 2025
923 Mw 7.7 Myanmar Earthquake: Implications for Geologically Controlled Seismic
924 Hazard. *Seismological Research Letters*, *97*(3), 1681–1696.
925 https://doi.org/10.1785/0220250388

926 Pitilakis, K., Riga, E., Anastasiadis, A., Fotopoulou, S., & Karafagka, S. (2019). Towards the
927 revision of EC8: Proposal for an alternative site classification scheme and associated
928 intensity dependent spectral amplification factors. *Soil Dynamics and Earthquake*
929 *Engineering*, *126*, 105137. https://doi.org/10.1016/J.SOILDYN.2018.03.030

930 Rahman, M. M., Bai, L., Li, H., & Liu, C. (2025). Probabilistic Seismic Hazard Map for
931 Bangladesh Including the Smoothed Background Seismicity and Local Site Effects.
932 *Pure and Applied Geophysics 2025 183:2*, *183*(2), 335–361.
933 https://doi.org/10.1007/S00024-025-03894-W

934 Rahman, M. Z., Hossain, M. S., Kamal, A. S. M. M., Siddiqua, S., Mustahid, F., & Farazi, A.
935 H. (2018). Seismic site characterization for Moulvibazar town, Bangladesh. *Bulletin of*
936 *Engineering Geology and the Environment*, *77*(4), 1451–1471.

https://doi.org/10.1007/s10064-017-1031-6

Rahman, M. Z., Kamal, A. S. M. M., & Siddiqua, S. (2018). Near-surface shear wave velocity estimation and V s30 mapping for Dhaka City, Bangladesh. *Natural Hazards*, *92*(3), 1687–1715. https://doi.org/10.1007/S11069-018-3266-3/METRICS

Rahman, M. Z., Siddiqua, S., & Kamal, A. S. M. M. (2015). Liquefaction hazard mapping by liquefaction potential index for Dhaka City, Bangladesh. *Engineering Geology*, *188*, 137–147. https://doi.org/10.1016/j.enggeo.2015.01.012

Rahman, M. Z., Siddiqua, S., & Kamal, A. S. M. M. (2016). Shear wave velocity estimation of the near-surface materials of Chittagong City, Bangladesh for seismic site characterization. *Journal of Applied Geophysics*, *134*, 210–225. https://doi.org/10.1016/j.jappgeo.2016.09.006

Rahman, M. Z., Siddiqua, S., & Kamal, A. S. M. M. (2021). Site response analysis for deep and soft sedimentary deposits of Dhaka City, Bangladesh. *Natural Hazards*, *106*(3), 2279–2305. https://doi.org/10.1007/s11069-021-04543-w

Rao, D. G., Bhattacharya, G. C., Ramana, M. V., Subrahmanyam, V., Ramprasad, T., Krishna, K. S., Chaubey, A. K., Murty, G. P. S., Srinivas, K., Desa, M., Reddy, S. I., Ashalata, B., Subrahmanyam, C., Mital, G. S., Drolia, R. K., Rai, S. N., Ghosh, S. K., Singh, R. N., & Majumdar, R. (1994). Analysis of multi-channel seismic reflection and magnetic data along 13° N latitude across the Bay of Bengal. *Marine Geophysical Researches*, *16*(3), 225–236. https://doi.org/10.1007/BF01237515/METRICS

Rathje, E. M., Kottke, A. R., & Trent, W. L. (2010). Influence of Input Motion and Site Property Variabilities on Seismic Site Response Analysis. *Journal of Geotechnical and Geoenvironmental Engineering*, *136*(4), 607–619. https://doi.org/10.1061/(ASCE)GT.1943-5606.0000255

Samm-A, A., Kamal, A. S. M. M., Hossain, M. S., & Rahman, M. Z. (2025). Probabilistic seismic hazard mapping for Bangladesh using updated source models. *Geomatics, Natural Hazards and Risk*, *16*(1). https://doi.org/10.1080/19475705.2025.2454537

Seed, H. B., Lysmer, J., & Schnabel, P. B. (1972). *SHAKE - A Computer Program for Earthquake Response Analysis of Horizontally Layered Sites | Resolution Copper Project and Land Exchange Environmental Impact Statement, Report No. EERC 72-1*. https://www.resolutionmineeis.us/documents/schnabel-lysmer-seed-1972

968 Shehab, M. U. (2015). *Evaluation oF dynamic properties of Dhaka subsoil for ground*
969 *shaking assessment*.
970 http://lib.buet.ac.bd:8080/xmlui/bitstream/handle/123456789/3419/Full
971 Thesis.pdf?sequence=1&isAllowed=y

972 Singh, A., Bhushan, K., Singh, C., Steckler, M. S., Akhter, S. H., Seeber, L., Kim, W. Y.,
973 Tiwari, A. K., & Biswas, R. (2016). Crustal structure and tectonics of Bangladesh: New
974 constraints from inversion of receiver functions. *Tectonophysics*, *680*, 99–112.
975 https://doi.org/10.1016/j.tecto.2016.04.046

976 Small, C., Steckler, M., Seeber, L., Akhter, S. H., Goodbred, S., Mia, B., & Imam, B. (2009).
977 Spectroscopy of sediments in the Ganges–Brahmaputra delta: Spectral effects of
978 moisture, grain size and lithology. *Remote Sensing of Environment*, *113*(2), 342–361.
979 https://doi.org/10.1016/j.rse.2008.10.009

980 Steckler, M. S., Akhter, S. H., & Seeber, L. (2008). Collision of the Ganges-Brahmaputra
981 Delta with the Burma Arc: Implications for earthquake hazard. *Earth and Planetary*
982 *Science Letters*, *273*(3–4), 367–378. https://doi.org/10.1016/j.epsl.2008.07.009

983 Steckler, M. S., Mondal, D. R., Akhter, S. H., Seeber, L., Feng, L., Gale, J., Hill, E. M., &
984 Howe, M. (2016). Locked and loading megathrust linked to active subduction beneath
985 the Indo-Burman Ranges. *Nature Geoscience*, *9*(8), 615–618.
986 https://doi.org/10.1038/ngeo2760

987 Street, R., Woolery, E. W., Wang, Z., & Harris, J. B. (2001). NEHRP soil classifications for
988 estimating site-dependent seismic coefficients in the Upper Mississippi Embayment.
989 *Engineering Geology*, *62*(1–3), 123–135. https://doi.org/10.1016/S0013-7952(01)00057-
990 6

991 Street, R., Woolery, E., Wang, Z., & Harik, I. E. (1997). Soil classifications for estimating
992 site-dependent response spectra and seismic coefficients for building code provisions in
993 western Kentucky. *Engineering Geology*, *46*(3–4), 331–347.
994 https://doi.org/10.1016/S0013-7952(97)00010-0

995 Szeliga, W., Hough, S., Martin, S., & Bilham, R. (2010). Intensity, Magnitude, Location, and
996 Attenuation in India for Felt Earthquakes since 1762. *Bulletin of the Seismological*
997 *Society of America*, *100*(2), 570–584. https://doi.org/10.1785/0120080329

998 Theodoulidis, N., Cultrera, G., Cornou, C., Bard, P. Y., Boxberger, T., DiGiulio, G., Imtiaz,

A., Kementzetzidou, D., Makra, K., Andreou, C., Bauz, R., Bayle, S., Bindi, D., Cara, F., Cogliano, R., Cretin, C., Fodarella, A., Günther, E., Konidaris, A., … Savvaidis, A. (2017). Basin effects on ground motion: the case of a high-resolution experiment in Cephalonia (Greece). *Bulletin of Earthquake Engineering 2017 16:2*, *16*(2), 529–560. https://doi.org/10.1007/S10518-017-0225-4

Wu, Z., Sun, J., & Li, Y. (2026). An ambient-noise-based physics–data integrated framework for far-field basin ground motion simulation. *Bulletin of Earthquake Engineering 2026*, 1–30. https://doi.org/10.1007/S10518-026-02559-W

Zaman, A., Al Alim, M., Ahmed, Z., Ansary, M., Nur, S., Hore, S., Hore, R., & Ansary, M. A. (2026). Critical evaluation of BNBC seismic response spectrum for Chattogram using one-dimensional nonlinear site response analysis. *Discover Geoscience 2026 4:1*, *4*(1), 159-. https://doi.org/10.1007/S44288-026-00503-8

Statements & Declarations

Funding

This research was supported by the Special Research Grant (2025–2026) from the Ministry of Science and Technology, Government of the People's Republic of Bangladesh (Grant ID: SRG-252373).

Competing Interests

The authors declare that they have no known competing financial interests or personal relationships that could have appeared to influence the work reported in this paper.

Author Contributions

The study conception and design were performed by Atikul Haque Farazi and José Piña-Flores. Material preparation, data collection, analysis, and artworks were performed by Atikul Haque Farazi, and José Piña-Flores. Supervision was done by Atikul Haque Farazi, Md. Shakhawat Hossain, Nasim Ferdous, and Sukhen Goswami. Editing of the original draft was done by Atikul Haque Farazi, and José Piña-Flores, Md. Shakhawat Hossain, Nasim Ferdous, Sukhen Goswami, and Md Wabidur Rahman. The first draft of the manuscript was written by Atikul Haque Farazi and all authors commented on previous versions of the manuscript. All authors read and approved the final manuscript.

Data Availability

The ambient-noise HVSR data and shear-wave velocity (V_S) models used in this study are available in Farazi et al. (2023) (https://doi.org/10.1016/j.jappgeo.2023.104967). The seismic waveform data from the reference station SHL are publicly available through the Federation of Digital Seismograph Networks (FDSN) (https://www.fdsn.org/networks/detail/IN/). The earthquake records used as input motions were obtained from the U.S. Geological Survey (USGS) earthquake catalog (https://earthquake.usgs.gov/earthquakes/search/). All other data generated or analyzed during the current study are available from the corresponding author upon reasonable request.